TO STUDY THE EFFECT OF SILVER COATED SILICA AND COPPER OXIDE NANOFLUIDS ON HEAT TRANSFER PERFORMANCE OF A CAR RADIATOR

A

DISSERTATION

Submitted in partial fulfillment of the requirement for the award of degree of

Master of Engineering
In
Thermal Engineering

Thapar University, Patiala

Submitted By
Kashminder Singh Mehta
Roll No. 801583013

Under the supervision of
Dr.S.S.Mallick, Mr. Kundan Lal Rana
Associate Professor, Assistant Professor
Mechanical Engineering
Department, Thapar University, Patiala (147004)

JUNE 2017

CERTIFICATION

I, Kashminder Singh mehta, declare that this thesis, submitted towards fulfilment of the requirements for the award of Master's Degree in Thermal Engineering, in Mechanical Engineering Department of Thapar University, Patiala, is entirely my own work. This document has not been submitted for any degree in any other institution.

Kashminder Singh

Date : 1st May, 2017

KASHMINDER SINGH MEHTA
801583013
Thapar University
Patiala

This is to certify that above statement made by the candidate is correct and true to the best of my knowledge.

D.R. S.S. MALLICK
Associate Professor, M.E.D.
Thapar University, Patiala.

M.R. KUNDAN LAL RANA
Assistant Professor, M.E.D.
Thapar University, Patiala.

i

ACKNOWLEDGEMENT

I would like to express my deep sense of gratitude to Dr. S.S. Mallick, Associate Professor, Mechanical Engineering Department, Thapar University, Patiala, India & Mr. Kundan Lal Rana, Assistant Professor, Thapar University, Patiala, India for their invaluable suggestions, excellent supervision, constant encouragement, thought provoking discussions and unabashed inspiration in nurturing the work and during the preparation of manuscript

Throughout the research work. My sincere thanks to Dr. S. K. Mohapatra, Professor & Head and Dr. Satish Kumar, Assistant Professor, Mechanical Engineering Department, Thapar University, Patiala, India for providing me with the opportunity to conduct this work and bring it out in the present form.

I offer my special regards to all my friends for providing their immense support in my experimental work throughout my research.

I am grateful to Mr. Harcharan, Laboratory Attendant, Department of Mechanical Engineering, Thapar University, Patiala for providing me all the lab facilities for the successful completion of my thesis work.

Above all, I thanks GURU GRANTH SAHIB, for all his blessings and kindness.

Kashminder Singh

ABSTRACT

Nanofluids are the suspension of nanoparticles in the base fluid. Nanofluids having the anomalously high thermal conductivity makes them the promising fluids for enhancing the heat transfer. At present, there is still some significant incongruity in thermal conductivity data of the nanofluids in the literature. At the same time, mechanisms of thermal conductivity enhancement of the nanofluids are still not understood. The Experimental studies presented over here is in terms of altering the properties of nanofluids such as: thermal conductivity, specific heat, density and viscosity of nanofluids with the change in concentration of nanofluids. The Enhancement mechanisms proposed for explaining nanofluid thermal conductivity are also summarized. Some discrepancies between the predicted data from the thermal conductivity data and the experimental data have been indicated. Recent experiments on nanofluids have shown that the heat transfer enhancement surpass the thermal conductivity enhancement of nanofluids. Therefore, the obtained agreement is the indication of validity of experimental results. We concluded that the heat transfer coefficient and the nusselt no. of the nanofluids are higher than those of base fluid and they increase with increasing the particle concentration as well as the Reynolds number. For volume concentration 0.01% the enhancement of heat transfer coefficient of copper oxide as compared to the base fluid ranges between 9% and 32%. For 0.02% it ranges from 21% to 37%and for 0.03% it ranges between 14% and 31%. Whereas the enhancement in heat transfer coefficient of silver coated silica nanofluids as compared to base fluid for volume concentration 0.01% is from 26% to 46%, for 0.02% it is from 30% to 58% and for 0.03%, it is from 29% to 45% respectively. Also, the hike in heat transfer coefficient by using silver coated silica nanoparticles as compared to copper oxide nanoparticles comes out to be from 20% to 35%.

Moreover, the increase in thermal conductivity leads to an increase in the heat transfer performance whereas the viscosity increment of the fluid increases the boundary layer thickness, which decreases the heat transfer performance. So, at volume concentration ≤ 1.0vol%, the effect of thermal conductivity enhancement may overcome the effect of the viscosity increment.

TABLE OF CONTENT

LIST OF FIGURES

LIST OF TABLES

NOMENCLATURE

Re	Reynolds no.
K	Thermal conductivity, W/m K
A	Area of the tube
Q	Heat transfer rate, W
m	mass flow rate, kg/s
μ_{nf}	Viscosity of nanofluids
μ_f	Viscosity of fluid
C_p	Specific heat, J/kg K
h	Heat transfer coefficient, W/m^2 K
Pe	Peclet number
Pr	Prandtl number
D	Pipe diameter, m
U	Average inlet velocity, m/s
Nu	Nusselt number
T	Temperature,°C
$\propto_{nf}$	Thermal diffusivity of the nanoparticles
ΔT	Temperature difference
T_b	Average inlet and outlet temperature
T_W	Average wall temperature

Chapter 1

Introduction

1.1 Need to Enhance the Heat Transfer

Heat transfer plays an important role in many applications. For example, heat generated by the prime mover in the vehicles needs to be removed for proper functioning. Air conditioning systems also includes several heat transfer processes. Heat transfer is also a key process in thermal power stations. Increasing the efficiency is very desirable because by increasing efficiency not only the associated power consumption will be minimized but also the space occupied by the radiator will be minimized. There are different methods available for improving the heat transfer efficiency. Some methods make use of extended surfaces, vibration for transferring heat and some use micro channels. Another method of improving the heat transfer efficiency is by increasing the thermal conductivity of the working fluid. The fluids which we use commonly for heat transfer fluids such as water, ethylene glycol, and engine oil have very low thermal conductivities, as compared to the thermal conductivity of solids. So, here we can use the high thermal conductivity of solids for increasing the thermal conductivity of a fluid by adding nano-sized solid particles to that fluid.

1.2 Introduction to Radiator

Basically radiators are heat exchangers which uses convection and radiation both the modes of heat transfer for cooling internal combustion engines, mainly the radiators are used in automobiles but they may also be used in piston-engine, aircraft, railway locomotives, motorcycles etc.

Engine coolant is being circulated through engine block for cooling the internal combustion engines. In engine block, the coolant gets heated up and then it loses its heat to the atmosphere in the radiator and returns back to the engine. Commonly, a water pump is employed to force the engine coolant to circulate. Some of the common applications of the car radiator are:

(1) Cooling automatic transmission fluids

(2) Cooling air conditioner refrigerant, intake air,

(3) To cool motor oil or power steering fluid.

1.3. Nanofluids

1.3.1. Introduction

With the recent improvements in the field of nanotechnology, these nano-sized (nanometer sized) particles can be produced with an ease. So, consequently this idea of suspension of nanoparticles in the base fluid for improving thermal conductivity has been recently proposed. As a consequence, the idea of suspending these nanoparticles in a base liquid for improving thermal conductivity has been proposed recently. These suspensions of nanoparticles in base fluid are called a nanofluid. The small size of nanoparticles enables them to easily fluidize within the base fluid, so the problems like clogging and erosion within the channel have also been vanished. Nanofluids can be used in microchannels as well.For good stability of the nanoparticles i.e. sedimentation of the particles can be avoided by utilizing proper dispersants.

1.3.2. Particle Material and Base Fluid

Different particle materials are used for nanofluid preparation for e.g. Al_2O_3, CuO, TiO_2, SiC, TiC, Ag, Au, Cu, and Fe nanoparticles. The need of carbon nanotubes is aroused where an exceptionally high thermal conductivity is needed in the longitudinal (axial) direction. The commonly used base fluids for preparing nanofluids are water, ethylene glycol and engine oil; these are the one which we use commonly as working fluid. For further improvement of the stability of the nanoparticles inside the base fluid, we need to add some additives i.e. surfactants apart from utilizing the proper dispersion methods.

1.3.3. Particle Size

Usually, the nanoparticles having diameter less than or below 100nm are used for the preparation of nanofluids. Moreover, particles having size less than 10nm have also been used by researchers. The non-spherical particles i.e. rod shaped particles, the diameter is less than 100nm but their length may be of some micrometer. Also, the particles may form clusters of the order of some micrometers due to the clustering phenomenon.

1.3.4. Particle Shape

Mostly the spherical shaped particles are used for nanofluids. However, the use of rod-shaped, disk-shaped and tube-shaped nanoparticles have also been seen. Also, the nanoparticles clusters formed in the base fluid may have fractal- like shapes.

1.3.5. Production Methods

1.3.5.1. Production of Nanoparticles

Production of nanoparticles can be done either using physical synthesis or chemical synthesis. Yu et al. [2008] has given the common techniques for production of nanofluids as follows.
Physical Synthesis: Inert-gas-condensation technique, Mechanical grinding
Chemical Synthesis: Chemical vapor deposition, chemical Precipitation, micro-emulsions, spray pyrolysis, thermal Spraying.

1.3.5.2. Production of Nanofluids

Basically, there are two different methods for nanofluid production, i.e. one-step technique and the two-step technique. In two-step technique, first step is the production of nanoparticles and the second step is its dispersion. Two step method is more preferable when the mass production of nanofluids is required because at present, large quantities of nanoparticles can be produced by utilizing the inert gas condensation technique. The major drawback of using the two-step technique is formation of clusters during the preparation of the nanofluids which interferes with the dispersion of the nanoparticles in base fluid.

In One-step technique, both the production and dispersion of nanofluids are done in a single step. However, this technique includes some variation. In the technique named direct evaporation one-step method, the nanofluid is produced by the solidifying the nanoparticles, which are initially the gas phase, inside the base fluid. The dispersion attribute of nanofluids produced using one-step techniques are much better than those which are produced using two-step technique. The major drawback of one-step techniques is that it is not suitable for mass production, which limits their commercialization.

1.4. Thermal Conductivity of Nanofluids

Studies towards the thermal conductivity of nanofluids reveals that a good enhancement of thermal conductivity can be obtained using nanofluids. An increment of more than 20% can be obtained at a very small particle volume fraction of 5% or even smaller. These enhancement values have surpassed the theoretical model predictions. This indicates the presence of the additional thermal transport enhancement mechanism of nanofluids.

Many experimental and theoretical studies have been carried out in the literature concerning the thermal conductivity of nanofluids. In further chapters, a detailed investigation of these studies have been shown and experimental data is compared with that of theoretical models of nanofluid thermal conductivity.

1.5. Heat Transfer Enhancement with Nanofluids

Increasing the thermal conductivity of the working fluid enhances the efficiency of the concerned heat transfer process. While considering the force convection inside the tubes, it is expected that the heat transfer coefficient enhancement and the thermal conductivity enhancement must be equal while using a nanofluid as directed by the definition of the Nusselt number. However, research regarding the heat transfer coefficient shows that the enhancement of heat transfer coefficient exceeds the enhancement of thermal conductivity of nanofluids. Several models were developed by researchers for explaining this extra enhancement.

1.6 Computational Fluid Dynamics

Computational fluid dynamics (CFD) is a tool for solving mathematical equations and models which governs the fluid flow. In most cases, the fluid flow involves mass transfer, heat transfer, phase change and chemical reaction etc. CFD is involves many disciplines as shown in figure 1.1. To solve any problem using CFD one should be well verse with either numerical analysis or mathematical modelling, fluid mechanics and computer science. CFD firstly converts the governing integral or differential equation into algebraic equations and then solves them using high speed computers.

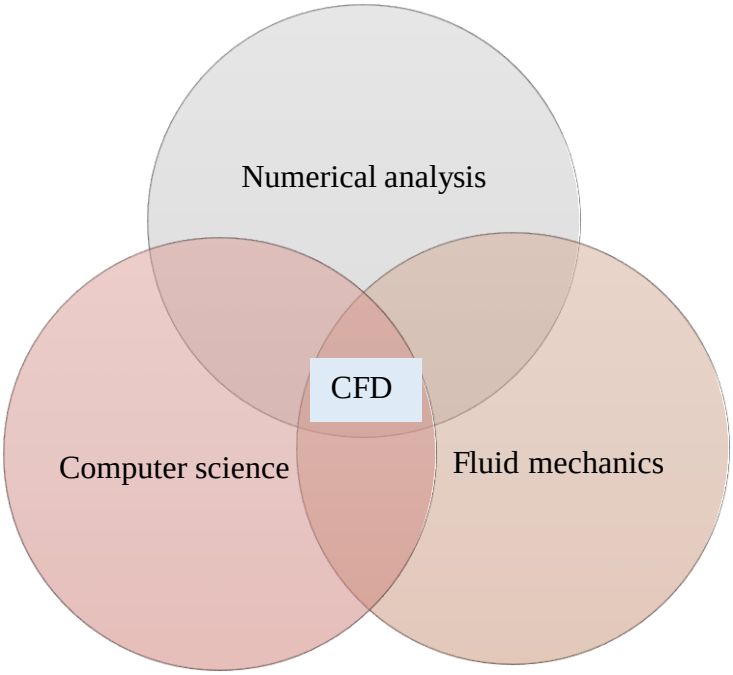

Figure 1.1: CFD an interdisciplinary branch

CFD applications involves,

1. Power plants
2. Environmental engineering
3. Sports
4. oceanography
5. IC engines
6. Weather predictions

1.6.1 Methodology of CFD

CFD involves the following process

1. Pre- processing
2. Solving
3. Post- processing

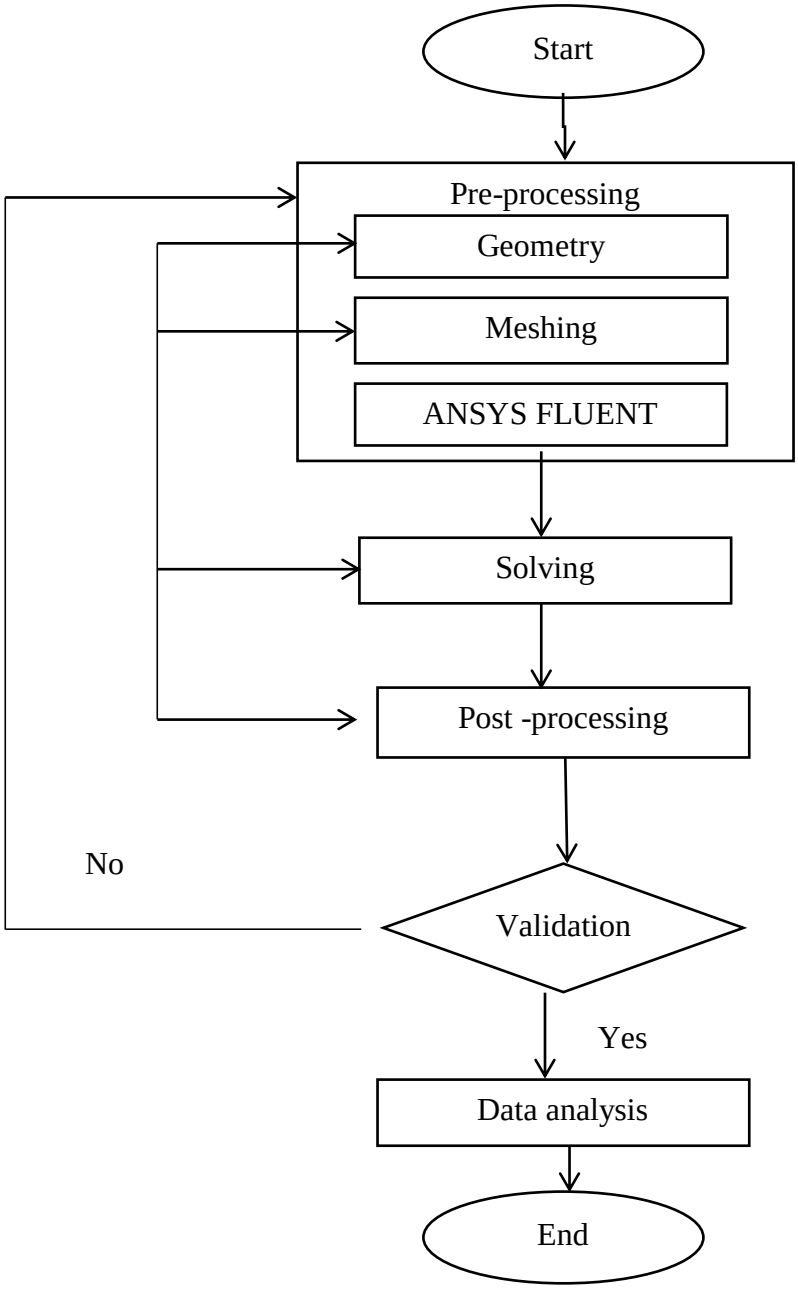

Figure 1.2 Steps involved in CFD represented in a flow chart

1. Pre-processing:

The first step in CFD is pre-processing

- First of all geometry is defined
- Then the geometry is meshed i.e. it is divided into small elements
- Then the inlet, outlet and wall conditions are defined
- At last the boundary conditions are stated.

2. Solving:

   In this step the governing equations of the fluid flow are solved by the following steps.

- Firstly, the governing equations are converted into the algebraic equations. This is called discretization.
- Then these algebraic equations are solved.

3. Post-processing:

   Post-processing provides the results of the problem i.e. Plots, graphs, contours and numerical values. The CFD results are not much reliable as they involve many approximations. Hence, the validation of CFD results is must with that of standard data or any experimental results obtained.

Chapter 2

Literature Review

Das *et al.* [2003] had investigated the two nanofluids i.e. Al_2O_3 and CuO in water as a base fluid. Thermal conductivity was measured using Temperature Oscillation technique. The alumina particles used were of the order of 38.4nm and CuO particles used were of the order of 28.6nm. Smaller size nanoparticles of Cuo shows a good enhancement of thermal conductivity. Thermal conductivity also increases with the increase in temperature and concentration.

Xuan *et al.* [2003] had investigated Cu nanoparticles having different concentration. The effect of changing concentration and different mass flow rates have been seen on heat transfer coefficient. It has been found that the heat transfer coefficient increases with an increase in particle volume fraction and mass flow rate. The Reynolds number was varied between 10,000 and 25,000. At higher concentration, the viscosity and heat transfer coefficient both increases. Also, at the same mass flow rate, the heat transfer coefficient of nanofluids was greater than that of base fluid. As the viscosity was increased, the energy transfer rate has also increased due to the fact that increased viscosity has decreased the turbulence. So, the random motion in the suspension has increased the energy transfer rate.

Jang *et al.* [2004] had investigated the mechanism behind the thermal conductivity of the nanofluids and found that Brownian motion plays a vital role in the enhancement of thermal conductivity of nanofluids. They have seen that it's not only the temperature and concentration of nanoparticles which effects the thermal conductivity but also the size of nanoparticles. Heat transfer in nanofluids takes place by four modes. (1) Collision between base fluid and nanoparticles molecules. (2) Collision due to the Brownian motion. (3) Thermal diffusion between the nanoparticles (4) Collision of base fluid molecules i.e. the conductivity of the base fluid. Brownian motion of the nanoparticles increases with the temperature, as the viscosity decreases with an increase in temperature. As the particle size of the nanoparticles decreases the random motion between the particles becomes immense and hence the convection effect become more dominant which in turn increases the thermal conductivity.

Murshed *et al*. [2005] had investigated two different nanoparticles having different shapes i.e. one was cylindrical having diameter 10nm and length 40nm and the other was spherical having diameter 15nm. The base fluid used was water. Transient hot wire method was used for the measurement of thermal conductivity and CTAB i.e. cetyl trimethyl ammonium bromide with very low concentration (0.01%-0.02%) was used. The thermal conductivity was enhanced by 30- 33% at a very small volume fraction of 5%. The surfactant used helped in proper dispersion of nanoparticles by hydrophobic surface force and strong electrostatic repulsive force. Smaller nanoparticles shows an enhancement in thermal conductivity. Also, the thermal conductivity increases with the particle size and concentration. The thermal conductivity of the cylindrical particles was found to be more than that of spherical particles.

W Evans *et al*. [2006] had investigated the Brownian motion and concluded that it has only a very small contribution in enhancement of thermal conductivity i.e. less than 1%. As in Brownian motion, they have assumed that the entire fluid and the nanoparticles have the same velocity and the suspension of the nanoparticles is uniform in the base fluid i.e. both the nanoparticles and the fluid are diffused together. Contribution in conductivity enhancement in the Brownian motion is given by,

$K_B = D_B C_P$, Where C_P is the heat capacity per unit volume, and D_B is the thermal diffusivity of the nanoparticles and K_B is the contribution of conductivity by Brownian motion.

$K_F = D_F C_P$ Where K_F is the conductivity, D_F is the diffusivity and C_P is the heat capacity of the fluid.

The very small value of this ratio i.e. $\frac{K_B}{K_F}$ Shows that the contribution of Brownian motion is negligible at low concentration.

Hong *et al*. [2006] had investigated the physics behind the clustering of nanoparticles. They used Fe nanoparticles for this purpose and observed that increasing the sonication time increases the thermal conductivity of nanofluids eventually. They also concluded that using the nanoparticles at higher concentration may lead to agglomerate formation more easily because the distance between the nanoparticles gets reduced.

Michel P. Beck *et al*. [2009] had investigated the alumina particles in water and ethylene glycol as base fluid. The results show that the nanoparticles having size smaller than 50 nm decreases the thermal conductivity. The correlations which shows the dependency of the particle size on the thermal conductivity is given as:

$$\in = \frac{K-K_1}{K_1} = \in_{max}(1- e^{-0.025d}) \quad (2.1)$$

$$\in_{max} = 4.4134\emptyset \quad (2.2)$$

$$\in_{max} = 5.527\emptyset \quad (2.3)$$

Where K_1 is the thermal conductivity of the base fluid, K is the thermal conductivity of the nanofluids, $\in_{max}$ is limiting value of the thermal conductivity. The equations (2.1) and (2.2) are valid only for the nanoparticles having ethylene glycol and water as a base fluid.

Madhursee Kole *et al*. [2010] had used smaller size nanoparticles i.e. less than 50 nm of Al_2O_3 Here the surfactant used was oleic acid and the nanofluids were kept for 80days to stabilize. The temperature of nanofluids was set between 10°C and 50°C. The increment in temperature has led to decrease in viscosity whereas the increment in concentration of nanoparticles has led to the increase in viscosity. A non-newtonian behavior of alumina has been observed at low concentrations for nanoparticles but Newtonian behavior has been observed for the base fluid that is pure engine coolant. The viscosity of nanofluids can be expressed as

$$log(\mu_{nf}) = \text{Aexp (BT)} \quad (2.4)$$

Leong *et al*. [2010] has investigated the car radiator using ethylene glycol and water as a coolant. Two different Reynolds number i.e. 6000 and 5000 have been used for air and coolant respectively. 3.8% enhancement was observed at a concentration of 2% of copper nanoparticles. While, only 0.9% enhancement was observed when using ethylene glycol as a coolant at Reynolds number of 4000 and 6000 for air and ethylene glycol respectively. Pumping power was also increased by 12.13% and area was reduced by 18.7%.

Tk Dey *et al*. (2010) had investigate a car engine using the coolant and Al_2O_3 nanoparticles having size less than 50nm nominal diameter. The surfactant used was oleic acid and the suspension was kept for more than 80 days at different temperatures ranging between 10°C and

80°C. An enhancement of 10.41% was obtained at room temperature. He also found that viscosity and thermal conductivity both were the function of concentration i.e. both the thermal conductivity and the viscosity increase as the concentration increases. The viscosity depends on the concentration based on the empirical correlation i.e. Log (μ_{nf}) = Ae^{-BT}. 11.25% was the maximum enhancement obtained at a concentration of 0.035 at 80°C.

A Vaisi *et al*. [2011] had investigated louveredfin compact heat exchanger. The dependency of geometric parameters on heat transfer and pressure drop has been seen. Results show that the pressure drop decreased by 18% and the heat transfer coefficient was enhanced by 9.3% at symmetrical arrangement. The weight of the fin has been reduced to 17.6% as louvers were more in number per row for symmetrical pattern. Pressure drop increases with an increase in air velocity for symmetrical pattern. Decreasing the number of fins has decreased the heat transfer area hence the cooling rate of fluid increases in case of symmetrical arrangement.

Peyghambarzadeh *et al*. [2011] had used smaller size nanoparticles i.e. of the order of 20nm in a mixture of ethylene glycol and water to investigate the performance of louvered fin radiator. The experiments were performed at five different concentrations i.e. 0.1, 0.3, 0.5, 0.7.1% vol of water and ethylene glycol and compared with that of pure ethylene glycol and water separately. The temperature ranges used were different for water (350- 500°C) and ethylene glycol (350- 600°C). Mass flow rate was varied from 2-6 L per min. Both the nanofluids show an increment of 40% in heat transfer coefficient. Results also show the slight dependence of temperature on heat transfer coefficient.

Peyghambarzadeh *et al*. [2011] had investigated an automobile radiator with Al_2O_3 nanofluids having a mean size of 20nm. Temperature was kept in a range of 37°C- 49°C. Whereas, the flow was set to be between 2- 5 L/min at five different concentrations of 0.1, 0.3, 0.5, 0.7, 1.0% vol. Results show that the temperature of coolant decreases with an increase in nanoparticle concentration. The mass flow rate of coolant increases with an increase in outlet temperature at same concentration. 45% enhancement was obtained at 1% vol. This is due to an increase in Nusselt number with Reynolds number.

Pramod *et al*. [2011] had investigated six different nanofluids having different shape and size. The thermal conductivity of the Nanofluid increases as the particle size increases. A theoretical model was given which shows the dependency of thermal conductivity on the particle size.

$$K_{eff}(L,T,\emptyset) \,/\, K_1(T) = [K_P\,(L,T) \,/\, K_1(\mathrm{T})]^{\emptyset} \qquad (2.5)$$

Where, $K_{eff}(L,T,\emptyset)$is the effective thermal conductivity of nanofluids as the function of temperature, particle size and concentration (L, T, $\emptyset$) respectively. $K_1(T)$ is the thermal conductivity of base fluid as a function of temperature. $K_P\,(L,T)$ is the thermal conductivity of particle as a function of temperature and particle size.

Murshed *et al*. [2012] had investigated two different nanofluids i.e. TiO_2 and AhO_3 using water as a base fluid. They had seen the effect of surfactant and agglomeration of nanoparticles in the base fluid on the thermal conductivity enhancement. Clusters are mostly formed when two-step process is used for formation of nanofluids. TEM (transmission electron microscope) was used for studying the cluster formation. It was observed that cluster formation or agglomeration increases with an increase in concentration, which in turn decreases the thermal conductivity of the nanofluids. Cluster formation depends on the shape, size, and viscosity of base fluid and concentration of the nanoparticles. After the cluster formation the free region between the nanoparticles increases which provides high thermal resistance, hence the thermal conductivity enhancement decreases. Two remedies were found to resist this cluster formation i.e. sonication and surfactants. Sonication break down the clusters and the stability of nanoparticles in the base fluid increases. So, the thermal conductivity of the nanofluids increases. Surfactants also increases the stability, the famous surfactant i.e. Cetyl trimethyl ammonium bromide (CTAB) is used in smaller concentration for stabilization and improving the dispersion in nanoparticles. The surfactant actually adsorbs on the surface of nanoparticles and increases the hydrophobic surface forces and electrostatic repulsive forces.

Reza Azizian *et al*. [2012] had investigated the mechanism behind the enhancement in thermal conductivity of nanofluids. He took 70nm Al_2O_3 nanofluids with water as a base fluid at a concentration of 13% by volume. He also took Tio_2 nanoparticles in water at a concentration of 5% by volume. It was found that the ballistic heat transport was the mechanism inside the small size particles for heat transport. It occurred due to two reasons i.e. the temperature gradient and the mean free path. Where mean free path according to Debye theory is

$$I = \frac{10\, a T_m}{\gamma\, T}$$

Where 'I' is the mean free path, 'a' is the lattice constant,'T_m' is the melting temperature, 'γ'bis gruneisen parameter and T is the temperature.

Arani *et al*. [2012] had investigated Tio_2 nanoparticles having size 30nm in deionized water. The Reynolds number was varied between 8,000 and 51,000. An increase in Reynolds number leads to an increase in Nusselt number but at the same time the power consumption also increases which in turn compensates the pressure drop. They found that for a given Reynolds number the nusslet number increases with an increase in particle volume concentration of the nanofluids. High concentration of nanofluids were used to examine the thermal performance therefore the nusselt number was also high.

Abdulhassn *et al*. [2012] had investigated three different nanoparticles of different sizes to see the effect on pressure drop and convective heat transfer coefficient. Those three nanoparticles were AI (25nm), AbO_3 (30nm) and Cuo (50nm). They have compared two different metal oxide nanoparticles and one metallic nanoparticle. The experimental conditions were set to be laminar in a circular tube. The experiments were performed for two different cases i.e.

a.) Test section with insulation

b.) Test section without insulation

An enhancement in nusselt number for the first case i.e. the test section with insulation for all the three nanoparticles was found to be 45%, 32% and 25% but at the same time the enhancement in nussselt number for the second case i.e. test section without insulation was found to be 36%, 23% and 19% for AI, AbO_3 and Cuo respectively. So, it was concluded that metallic nanoparticles show more rise than that of the oxide nanoparticles at the same particle concentration. Also, the smaller sized nanoparticles have shown greater rise in thermal conductivity as the random motion becomes more dominant in these particles and the convection comes into the play.

Naraki *et al*. [2013] had investigated car radiator under laminar flow i.e. having Reynolds number in the range of 100 to 1000. Results show an enhancement of 8% at a low volume concentration of 0.4% as compared to distilled water. The reason for this massive enhancement at such a small

concentration is the Brownian motion and thermal conductivity. Increment of flow rate has led to the heat transfer coefficient enhancement, but as the inlet temperature elevates the heat transfer coefficient falls. The reasons for this fall are a.) Due to the increase in temperature the viscosity of nanofluids decreases more than its density which results in higher Reynolds number. b.) As the viscosity of nanofluids is low so the particle alignment becomes more rapid which leads to the less contact between nanoparticles. C.) Thermal conductivity decreases as the particles diminish near to the wall surface.

Adnan M. Hussein *et al.* [2013] had investigated the tube cross sectional effect on the heat transfer of car radiator for improving the cooling performance of the car radiator. The CFD model was prepared with fluent software using finite volume technique. The investigation was done with three different shapes and for different concentration of tio_2 nanoparticles i.e. 1%, 1.5%, 2%, and 2.5%. Different cross sections were also considered i.e. elliptical, circular and flat type having length of 500mm and hydraulic diameter of 3mm. The friction factor for circular tube was found to be higher than those of flat and elliptical tube. Decrement of friction factor with an increase in Reynolds number has also been observed. Hence, the flat tube has the highest heat transfer coefficient followed by the elliptical and then the circular cross section. This is because the flat tube has the highest cross sectional area followed by the elliptical and then the circular tubes.

Jahar sarkar *et al*. [2013] had used ethylene glycol/water mixture in the ratio of 20% (ethylene glycol) and 80% (water). He tried to improve of the cooling capacity, effectiveness and reduction in pumping power using four types of nanoparticles i.e. SiC, Cu, $Al_2o_3$and ti$o_2$in coolant as base fluid. Results show that the cooling capacity has given the maximum enhancement for Sic followed byAl_2o_3, ti$o_2$and then Cu respectively. Maximum enhancement obtained was 15.34% for Sic, for Al2o3it was 14.33%, for ti$o_2$it was 14.03 and 10.20% for Cu. Increasing the mass flow rate also, increases the cooling capacity. This is due to the decrease in effectiveness and increase in heat transfer coefficient. It was found that Cu based nanofluid has least effectiveness and cooling capacity as compared to others. Also, increase in mass flow rate increases the effectiveness and cooling capacity. Pumping power required for Cu was also less than others while increasing the inlet temperature of nanofluids. A small increment in effectiveness but a good increment in heat transfer coefficient has been seen. Second law efficiency and effectiveness was increased for each nanofluid.

Tun- ping teng *et al*. [2013] had investigated a performance of bike radiator using carbon nanotube at three different concentrations i.e. 0.1, 0.2, 0.4 wt% and used ethylene glycol and cationic dispersant equally. All thermo physical properties were studied at four different temperatures i.e. 95°C, 90°C, 85 °C and 80°C and at three mass flow rates i.e. 8.5, 6.5, 4.5 L/min. Also, investigated the relation between the heat exchanger capacity and pumping power using efficiency factor and efficiency. 12.8% of enhancement was obtained in heat transfer, 4.9% in pumping power and 14.1% in efficiency factor respectively.

Peyghambarzadeh *et al*. [2013] investigated the car radiator using two nanofluids i.e. Fe_2O_3 and CuO at single mass flow rate of 10 L/min but different concentrations. The obtained data was compared with that of De- ionized water and the theoretical relations of heat transfer. Results show that increasing Reynolds number of air also increases the heat transfer coefficient. But keeping the Reynolds number and concentration same and increasing the temperature decreases the heat transfer coefficient.

Navid Bozorgan *et al*. [2013] had investigated the automotive diesel radiator using Al_2o_3nanofluids in water with a mean size of 20nm. The experiments were performed under turbulent conditions. Results show that the increasing the speed of vehicle decreases the pumping power at same concentration but at varying concentrations the pumping power increases with increasing concentration at constant speed. As the concentration increases the density and viscosity of nanofluids also increases which increases the pressure drop, which further increases the friction factor.

LotfizadehDehkordi *et al*. [2013] had done experiments using ethylene glycol and water in the ratio 60:40 as a base fluid and Al_2o_3 as nanoparticles. The effects of concentration of surfactant SDBS on thermal conductivity and viscosity has been seen. The concentration < 1 wt% of the surfactant SDBS gives a good enhancement in thermal conductivity and good dispersion too. But as the concentration of the surfactant goes above > 1 wt% the thermal conductivity is decreased and the nanoparticles starts settling due to the enhanced viscosity of the nanofluids. Also, the higher concentration of surfactant leads to inter molecular forces and produces foam, which in turn decreases the thermal conductivity of nanofluid. The thermal conductivity of nanofluids increases with an increase in temperature and concentration.

Hwa-Ming Nieh *et al*. [2014] had investigated an air cooled radiator using two different nanofluids i.e. $Al_2O_3$and tiO_2. Other properties like viscosity, thermal conductivity and specific heat were also measured at different volume fraction. Results show the relation between the heat dissipation capacity and pumping power using efficiency factor. Both the heat dissipation and the efficiency factor are higher for nanocoolant as compared to ethylene glycol/water mixture. Enhancement obtained in Tio_2 was greater than those of Al_2O_3. Enhancement of 25.6%, 6.1%and 27.2% were obtained for heat dissipation rate, pressure drop and efficiency factor respectively.

Durgeshkumar chavan *et al*. [2014] Comparison of Al_2O_3nanofluids and pure water have been done to analyze the enhanced heat transfer performance of radiator using nanofluids. Range for mass flow rate was set from 3L/min to 8L/min and the flow was turbulent. Nanoparticles were used with concentrations between (0-1) volume percent. Results showed that the heat transfer performance increases with flow rate. 40-45% of enhancement is obtained in heat transfer performance as compared to pure water at 1% volume concentration. Also, as the particle size was reduced the Brownian motion effect comes into picture and the heat transfer rate of nanofluid has increased because of this random motion.

Vermahmoudi Y *et al*. [2014] had investigated the laminar flow condition using Fe_2O_3/waternanofluids.The mass flow rate was kept between 0.2 to 0.5 m^3/ hr at three different temperatures i.e. 50°C, 60°C and 80°C and also at three different particle volume fractions i.e. 0.15%, 0.40% and 0.65% by volume. The Reynolds number was varied from 200 to 1000. With the increase in Reynolds number, the heat transfer coefficient is also increased but when the Reynolds number is kept constant, then by increasing the volume concentration of nanoparticles, the heat transfer coefficient increased. Air side Reynolds number was kept from 400 to 700. As the movement of air started, increasing the heat transfer coefficient has also started increasing due to the increment in the energy transfer from nanofluid to air. 13% enhancement is obtained here using only 0.65% concentration of nanoparticles as compared to the distilled water.

Adnan M. Hussein *et al*. [2014] had investigated the SiO_2/water nanofluid to see the effect on heat transfer enhancement and friction factor, experimentally and numerically. Mass flow rate was kept somewhat high i.e. from 21/min to 81/min and the concentrations were in the range from 1 to 2.5 vol%. Reynolds number was kept between 500 and 1750. With the increase in mass flow rate

the friction factor decreases whereas the nusselt number increases. But both the heat transfer coefficient and friction factor increases with the increase in particle volume concentration. At volume concentration of 2.5% an enhancement of 22% and 40% has been observed in friction factor and nusselt number respectively.

Sandesh S. Chougle et al. [2014] had investigated the performance of car radiator using two nananofluids i.e. carbon nanotubes (CNT) and Al_2o_3nanoparticles with water as a base fluid. Concentration ranges between 0.15 and 1 vol%, whereas a high mass flow rate of 21/min to51/min has been used. The experimental set up was of forced convection heat transfer and the enhancement of 90.76% and 52.03% was obtained for CNT and Al_2O_3 respectively. Also, as the mass flow rate increases the heat transfer performance increases respectively. The reason for enormous enhancement of CNT nanofluids as compared to the other one is its high thermal conductivity, low thermal resistance and high aspect ratio. With an increase in particle volume fraction, the thermal conductivity increases and hence, the cooling performance increases.

Chapter 3

Research Gaps and Objectives

3.1 Research Gaps

1.) More research is needed in the area of metal and oxide nanoparticles i.e. we can think to synthesize some material using metal and oxide particles in the form of nanofluids. So, as to get the more enhancement in thermal conductivity and heat transfer coefficient both.

2.) The major problem experienced in nanofluids is the stability of the suspensions. As strong Vander walls forces of attraction causes the formation of clusters within the base fluid. Many experiments were performed to overcome this problem by using additives and varying PH but it decreased the thermal conductivity due to the thermal resistance offered between the agglomerates. So, to improve the stability of nano-fluids in order to measure the thermo-physical properties for future applications some nanoparticles material must be chosen which may have the conducting as well as the insulated properties.

3.2 Objectives

1. To develop the experimental set up of car radiator.
2. To experimentally investigate and compare the performance of a radiator using two different nanofluids at different mass flow rates i.e. 3, 3.5, 5 lpm, different inlet temperatures i.e. 35℃, 40℃, 45℃ and different volume concentration i.e. 0.02, 0.05, 0.07 for both the nanofluids.
3. To evaluate the hike in heat transfer coefficient by using coated nanoparticles as compared to copper oxide nanoparticles.
4. To numerically investigate and compare the experimental using ANSYS Fluent.

Chapter 4

Preparation of Nanofluids

Nanofluids are basically the dispersion of small solid particles i.e. of the nano-size order in some base fluid like ethylene glycol, water, bio- fluids, glycols etc. Generally, we use either one step or two step method for the preparation of nanofluids. In one step method, we make and disperse nanoparticles simultaneously, whereas in two step method, we first prepare and then disperse the nanoparticles in the base fluid. We generally use two step method for the preparation of the nanofluids.

Synthesis of silver coated silica nanoparticles was done by my colloquies using reduction method and the copper oxide nanoparticles were bought. Before preparing the nanoparticles, the concentration was calculated by weight. After preparation, the nanoparticles were dispersed in the base fluid.The particle volume fraction of the nanoparticles to be added used calculated using the formula:

$$f_v = \frac{V_{np}}{V_{bf}+V_{np}} \quad (4.1)$$

Figure 4.1: Chemical balance apparatus.

The chemical balance apparatus as shown in fig. 4.1 was used to calculate the weight of nanoparticles.

After dispersion of nanoparticles, we need to treat the nanofluid in two equipments for the proper dispersion and stability of the nanoparticles in the base fluid. These equipments are

1. Magnetic Stirrer.
2. Ultrasonic vibrator.

4.1 Magnetic Stirrer

For the proper dispersion of nanoparticles in the fluid magnetic stirrer is used. The magnetic stirrer bead is placed in the nanofluids. After that, the flask having nanofluids is placed on the disk of the magnetic stirrer and stirrer is turned on. The speed of mixing can be controlled by using a dimmer provided on the apparatus. The magnetic base of the stirrer and the magnetic stirrer bead have different poles. So, when the stirrer is turned on the magnetic stirrer, bead starts rotating and the nanoparticles start dispersing properly inside the flask. The figure 4.2 below shows the magnetic stirrer and nanofluids present on it.

Figure 4.2: Magnetic stirrer.

After stirring, still there is a chance that nanoparticles will form agglomerate in the base fluid. So, to make sure that no agglomeration is formed, surfactants are used in nanofluids. Madhursee kole et al. (2010) suggested that for aluminium oxide oleic acid is best suited surfactant Duangthongsuk and Wongwises (2009) also investigated that the surfactant does not effects the thermo-physical properties of nanofluid when used at low concentration i.e. 0.01%. Hence, a low concentration of CTAB surfactant was used during the stirring. Magnetic stirrer was operated for 30 minutes for every concentration.

4.2 Ultrasonic Vibrator

After magnetic stirring, there is still a chance of cluster formation or occurrence of sedimentation. So, to avoid this the nanofluid are treated with sonication using ultrasonic vibrator. Ultrasonic vibrators are of many types but we have used bath type sonicator here as shown in Figure 4.3 and 4.4.

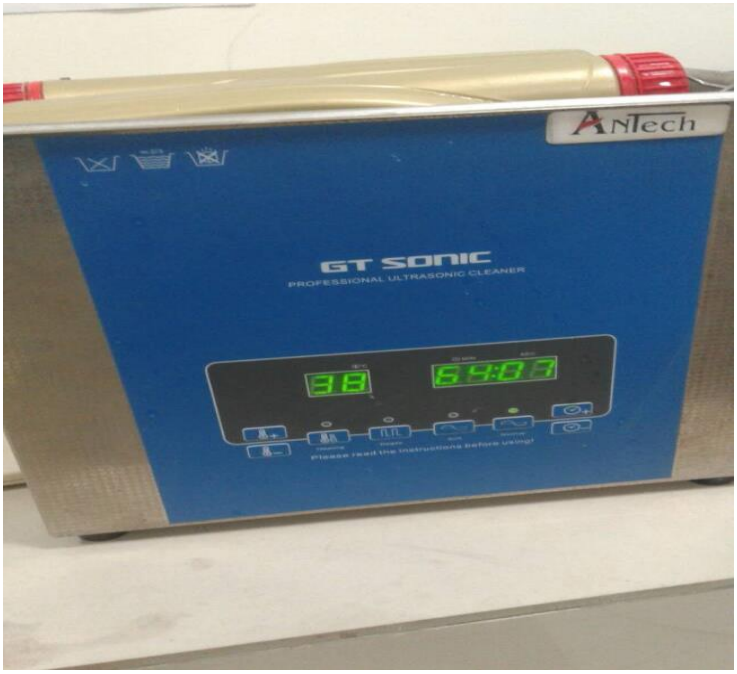

Figure 4.3: Ultrasonic Vibrator

The ultrasonic vibration was continued for 90 minutes for each concentration at room temperature. Basically, the ultrasonic vibrate breaks the clusters formed in the nanofluids using sound energy. The speed of the vibration can be set according to the need. Nanofluid preparation

in the ultrasonic vibrator is shown in the figure 4.4. and figure 4.5 shows the prepared nanofluids.

Figure 4.4 Ultrasonic Vibrator

Figure 4.5: Nanofluid prepared

Chapter 5

Measurement of thermophysical properties and Calibration

5.1 Thermo physical properties measurement

Different experiments have been conducted for measuring the thermo physical properties of the nanofluids i.e. thermal conductivity, viscosity, density and heat transfer coefficient using instruments like KD2 PRO for measuring thermal conductivity, Brookfield DV-3 for measuring viscosity and specific density gravity bottle for measuring density. Temperature measurement was done using data logger. Temperatures were measured at inlet, outlet and at the surface of the radiator.

5.1.1 Thermal conductivity measurement

The thermal conductivity of both the nanofluids are measured using KD2 Pro (Decan Devices, USA). The instrument has different sensors meant for different purposes. Here, KS-1 sensor needle was used for measuring the thermal conductivity. The sensor needle is made up of stainless steel having diameter of 1.3mm and length of 60mm. For having the accurate results the needle should be in same place i.e. it shouldn't be disturbed. The instrument was calibrated using the glycerin liquid available with the instrument set only and values were matched with the manual present inside the instrument set. The correctness in measurement was in the acceptable range of 0.3-3 w/mk which matches with that of ASTM56 and 1EEE57 standards. The thermal conductivity of water has also been measured and was checked against the standard data.

While performing the experiments, the needle was kept vertically in a tube using a holder. The gap between the two readings of the thermal conductivity should be at least 15 minutes. As the needle works by heating the liquid, so there is some time needed for cooling down. There is also an automatic mode present in the instrument which automatically measures the values and keep recording after a minimum time interval. Also, there comes an error value with every thermal conductivity value. The error value should be less than permissible value i.e. 0.0100 for every reading.

Fig 5.1 shows KD2 Pro thermal properties analyser

5.1.2 Viscosity measurement

The viscosity measurement was done using Brookfield DV-3 Rheometer. The instrument was calibrated using de-ionized water and the error between the readings was 1-2% which is acceptable. The instrument was connected to computer where all the values of viscosity were stored. The viscosity of the samples were measured at different concentrations and different temperatures i.e. at 35℃, 40℃ and 45℃. The device needs to be connected to the bath tub to vary the temperature of the fluid. The device needs to be cleaned after every sample reading.

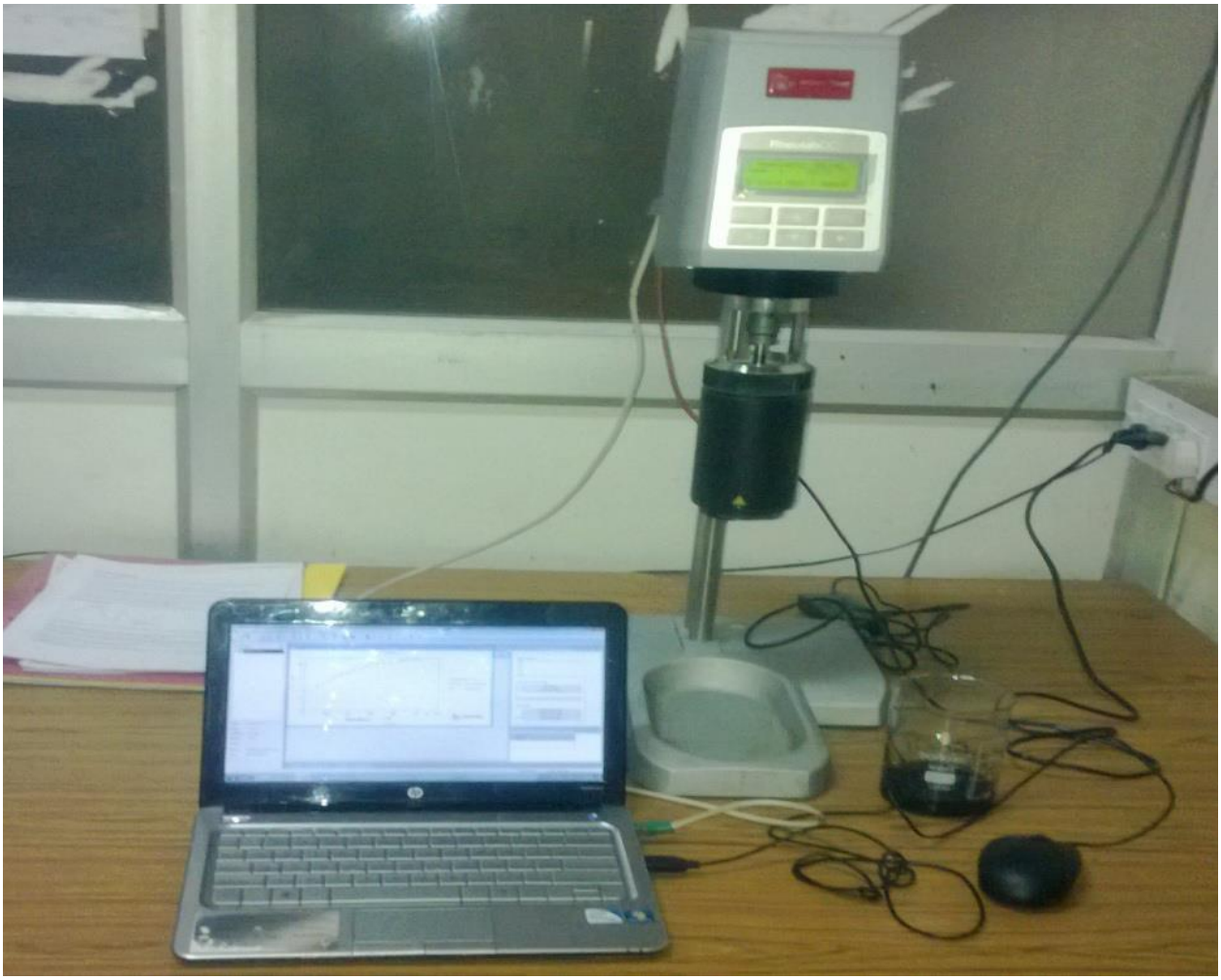

Fig 5.2 Brookfield DV-3 Rheometer

5.1.3 Specific gravity Bottle

The density is measured using specific gravity bottle. It consists of a bottle in which the liquid of unknown density is poured. Then, the bottle is weighed with and without the liquid. The difference between these two weights are then divided by the weight of an equal volume of water and the specific gravity of the liquid is obtained. Note that as water has the density of 1 g/cm^3, the specific gravity is the same as that of the density of the material in g/cm^3.

Fig 5.3 specific gravity bottle

5.1.4 TEM (Transmission Electron Microscope)

Transmission electron microscope is used for obtaining the smaller column of atoms and other objects in the light of microscope. TEM basically is used for getting high resolution images of the dispersion. It works on the principle that when the beam of light falls on sample and after getting transmitted, a magnified image is formed on detecting device. Tem images were taken from NIPER, Mohali. The image 5.4 shows the Transmission electron microscope and the figures 5.5

and 5.6 shows the Tem images of dispersion of silver coated silica nanoparticles and copper oxide nanoparticles.

Fig 5.4 Transmission electron microscope

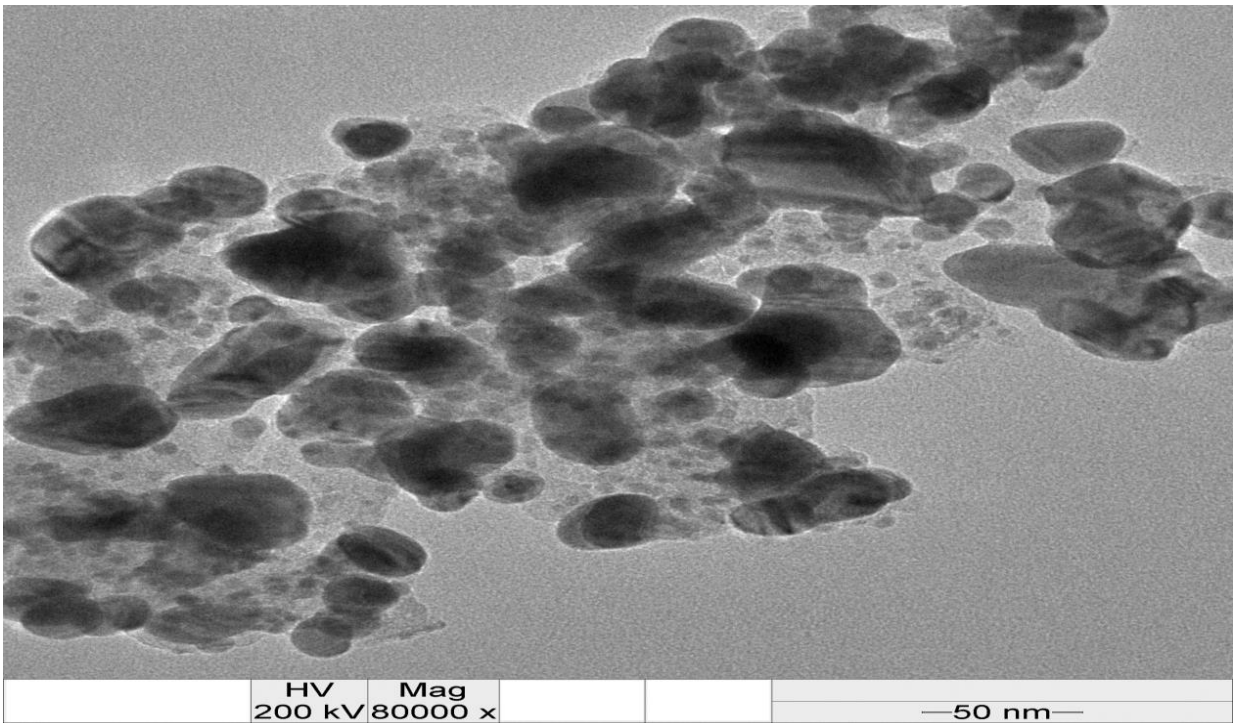

Fig 5.5 TEM image for silver coated silica nano-particles dispersed in base fluid

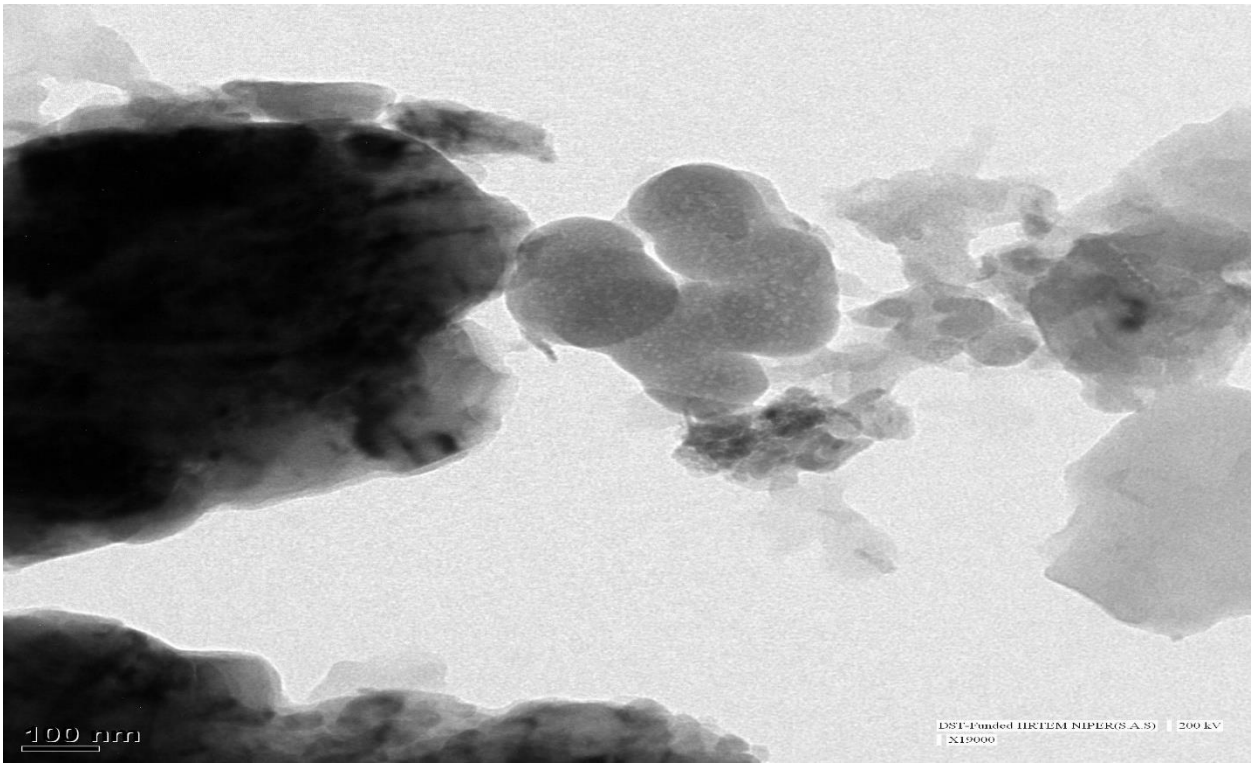

Fig 5.6 TEM image for Copper oxide nano-particles dispersed in base fluid

5.1.5 EDS (Energy Dispersive Spectroscopy)

This is a technique used for the detection of elements and the chemical composition. EDS is done for silver coated silica nanofluids. EDS also recognizes the contamination in the sample and its concentration on the surface. EDS was done at JEOL JSM-6510LB (SAI Lab, Thapar University, Patiala).

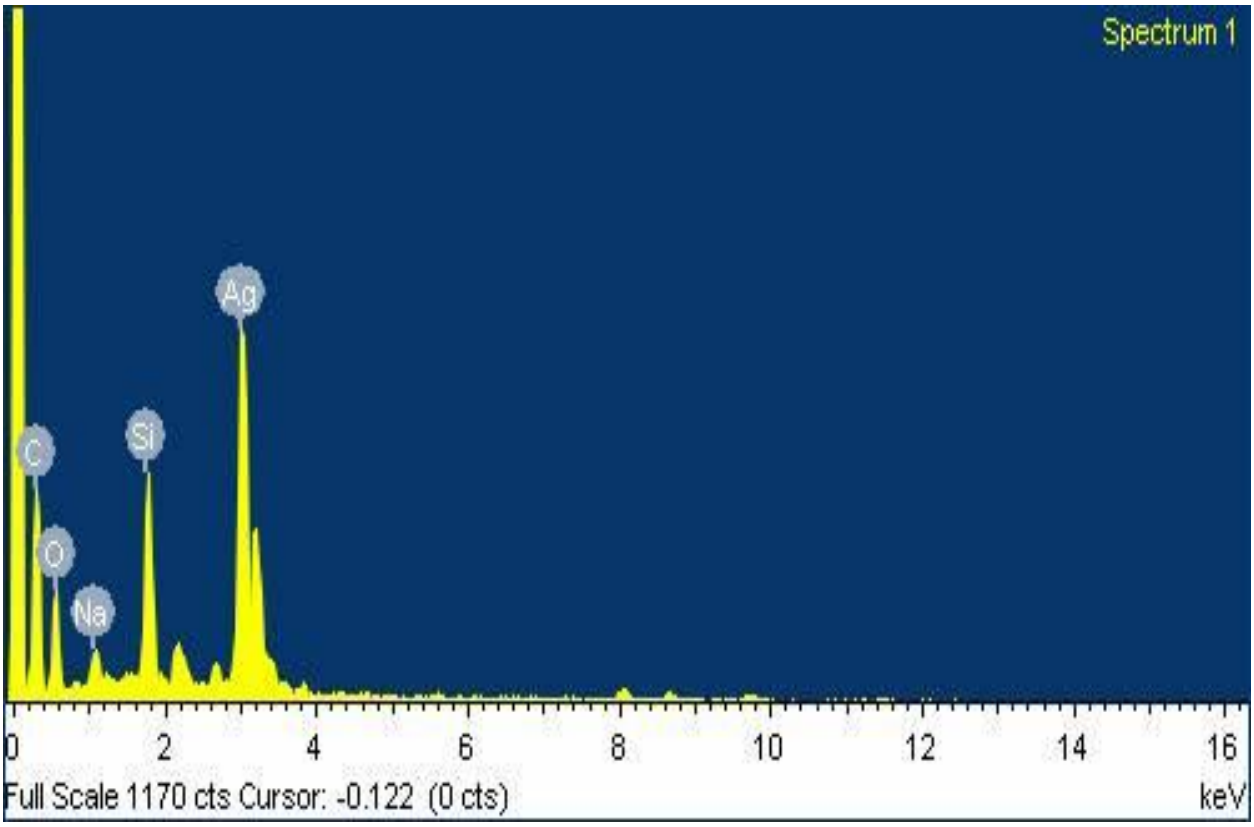

Fig 5.7 EDS image of silver coated silica nano-particles

5.2 Calibration

The calibration of thermocouples and rotameter have been done from NIIRT (National institute for industrial research and technology)

5.2.1 Calibration of Rotameter

The Rotameter is calibrated using a stop watch and a measuring beaker by NIIRT. Firstly, the calibration is done with water then with coolant and nanofluids. The time taken to fill the 1000ml fluid in the beaker is recorded and units are converted to ml/min.

S.no.	IUC Reading	STD Value(LPM)	Correction to IUC (LPM)	Uncertainty
1	3.0 lpm	2.92 lpm	-0.08	± 0.1 lpm
2	3.5 lpm	3.40 lpm	-0.10	
3	5.0 lpm	4.90 lpm	-0.10	

Table 5.1 calibration of Rotameter

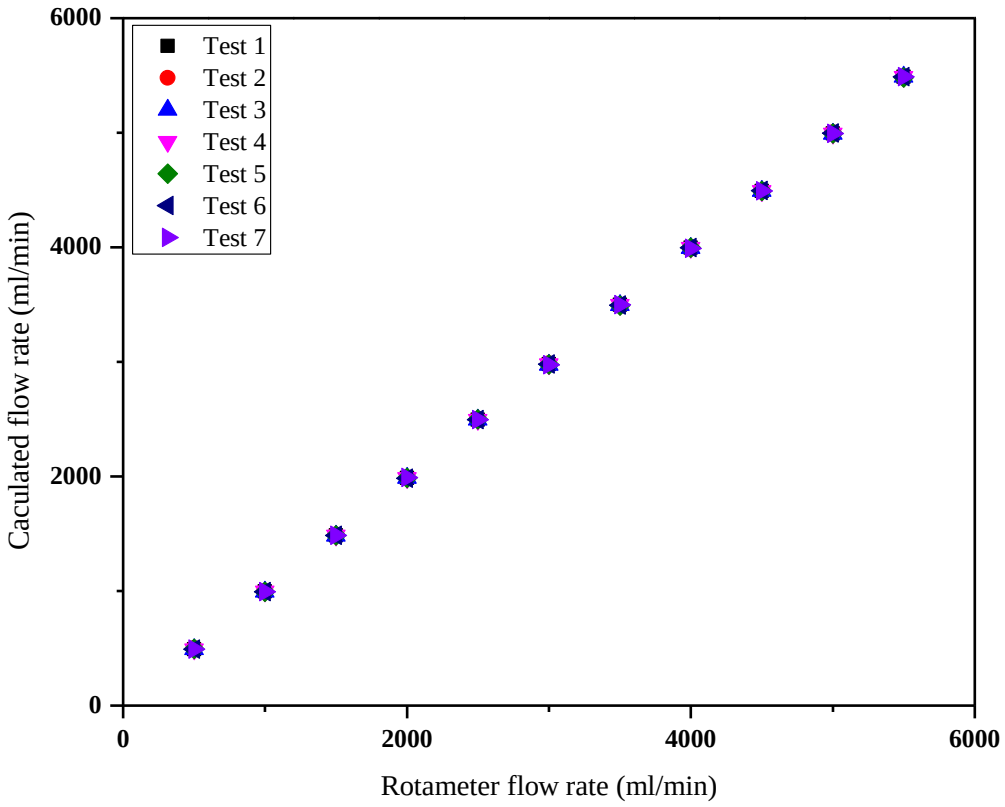

Fig 5.8 Calibration of Rotameter

5.2.2 Calibration of resistance temperature detection sensors (Rtd)

The calibration of Rtd sensors were calibrated using water bath. The sensors are dipped into water bath and are connected to data logger, the temperature of bath is varied and Rtds readings are compared with that of thermometer. The uncertainty is ±0.71.

S.no.	STD Temperature (°C)	IUC Temperature (°C)										Uncertainity(°C)
		CH0	CH1	CH2	CH3	CH4	CH5	CH6	CH7	CH8	CH9	
1	25.50	26.2	26.2	26.2	25.9	25.9	26.0	25.9	26.0	26.0	26.2	±0.71
2	40.51	41.1	41.1	41.1	40.8	40.8	40.8	40.7	40.7	40.8	40.8	
3	60.62	60.9	60.8	61.2	60.8	60.8	60.8	60.7	60.5	60.9	60.7	

Table 5.2 calibration of Rtds

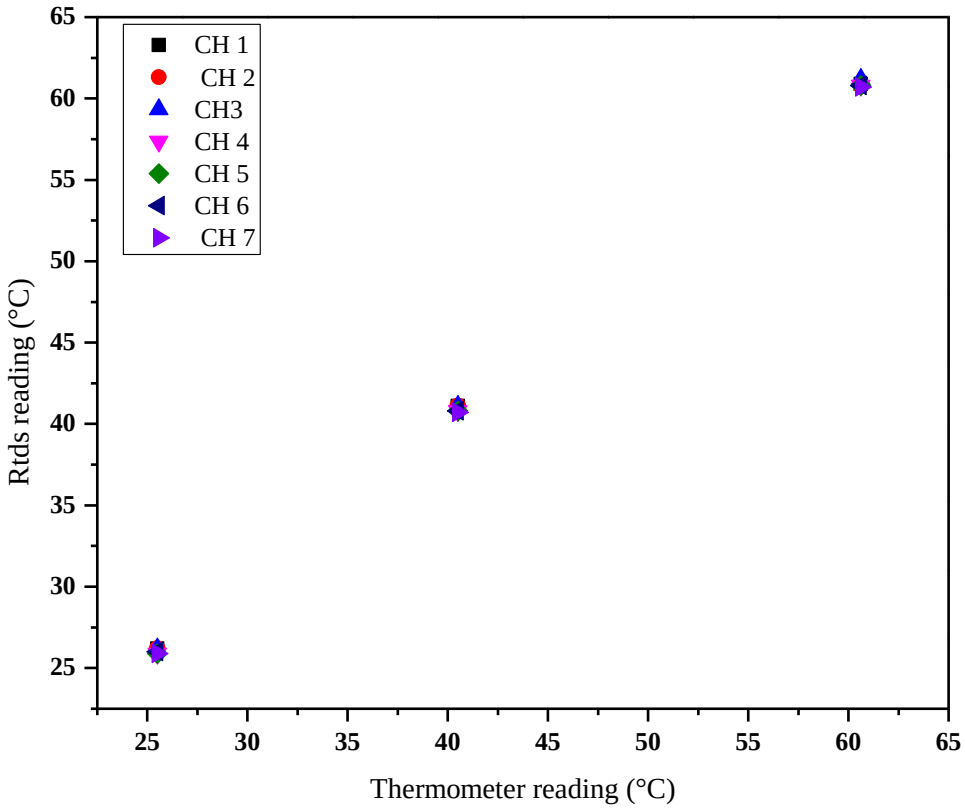

Fig 5.9 Calibration of Rtd sensors

Chapter 6

Experimental Setup and CFD Methodology

6.1 Experimental Setup

A radiator is used for conducting experiments as shown in Figure 6.1. Whereas, Figure 6.2 shows the schematic diagram of experimental setup.

Figure 6.1: Experimental setup

The experimental set up constitutes of the following essential components,

1. A car's radiator has been used for finding the heat transfer coefficients and all other parameters which affect the heat transfer coefficient of radiator. There are total 38 tubes present in the radiator covered by fins. The tubes are made up of aluminium. The dimensions of the radiator are as follows :

Inner diameter of aluminium tube: 8mm

Outer diameter of tubes: 10mm

Tube thickness: 2 mm

Tube spacing: 5 mm

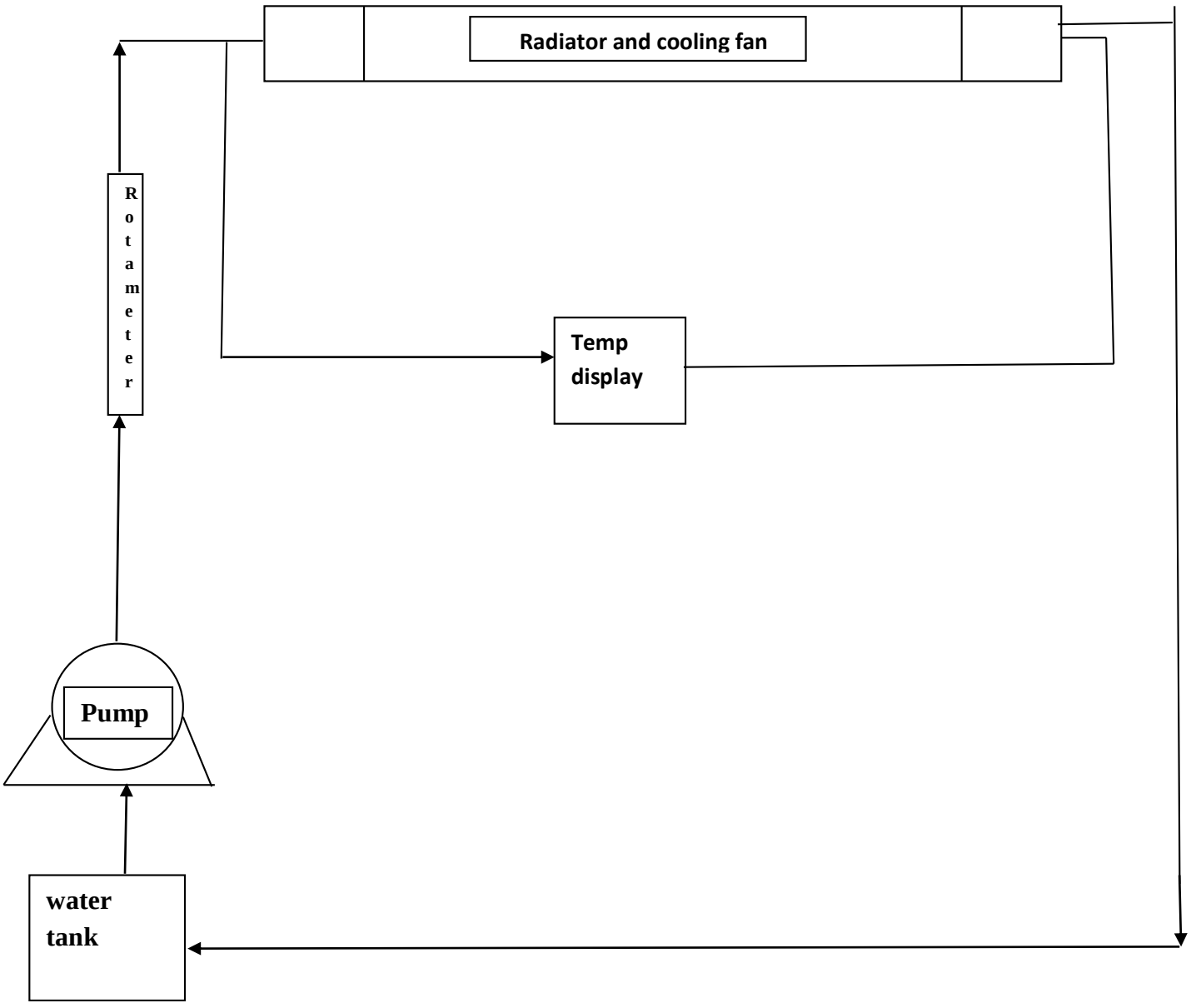

Figure 6.2: Schematic diagram of Experimental setup

2.) A water tank having a capacity of 20 litres is used. In order to minimize heat losses tank is covered with asbestos sheet followed by the aluminium tape. The radiator used for experimental purpose is shown in Fig. 6.3. The inlet temperature of the water was increased by using a heater element having a power of 3KW. The fluid is fed from the tank and after circulation the fluid returns back to the same tank.

Figure 6.3: Front view of Car radiator

Figure 6.4: Rear view of Car radiator

3. A centrifugal pump is used to feed water from tank and then back to the tank after circulation. Figure 6.5 shows a centrifugal pump used.
4. Rotameter is used to control the mass flow rate of the fluid. Rotameter was firstly calibrated with water and then with both the nanofluids used. Control valve provided on rotameter is used for changing the mass flow rate. Rotameter used is shown in Figure 6.6

Figure 6.5: Centrifugal Pump

Figure 6.6: Rotameter

5.) Since the fluid is circulated from and to the tank, the temperature of the fluid present in the tank changes. So, to avoid the temperature change and to maintain the constant temperature we used (PID) device i.e. Proportional Integral Derivative. A PID controller is installed and connected with heater, basically it consists of temperature sensor, temperature display and a provision to set the required temperature. The sensor of this PID controller is dipped in a tank containing fluid and

a required temperature is set. After the fluid reaches the required temperature, it sends the signal to the device and power is switched off. If the temperature falls below the set temperature, it again switches on the heater supply and maintain the required temperature. Figure 6.7 show the PID controller

Figure 6.7: PID controller.

6.) Temperature sensors are used for measuring the temperatures at different points. These sensors are of various types having different ranges of temperatures to be measured. In these experiments, we have used RTD´s i.e. Resistance Temperature Detectors are used. Total 10 different temperature sensors were used, two of which are attached to the inlet and outlet of the radiator and the rest eight were attached to the surface of the radiator. The surface temperature detectors are used to get the average wall temperature. All the ten sensors were having the maximum range of 100℃ and are attached to the data logger, from where the temperature readings were obtained. Figure 6.8 shows the data logger

Figure 6.8: Temperature Data logger

Figure 6.9: Heating element

Figure 6.10: Centrifugal pump

7.) Figure 6.9 shows the heating element used for heating the fluid in the tank. Figure 6.10 shows the centrifugal pump installed inside the tank. So, as to avoid the formation of agglomerates during the experiments.

6.2 CFD Modelling

Computational Fluid Dynamics (**CFD**) is the art of replacing such PDE systems by a set of algebraic equations which can be solved using digital computers. CFD is used here for validating the experiments. The CFD results are compared with the experimental results. The following steps were followed for CFD analysis:

1. First of all a geometry is modelled for defining the zone of CFD analysis. The modelling is done in Ansys Design Modeller
2. Then the Meshis generated where the geometry is divided into grids. The mesh is generated in Ansys Mesher
3. Choosing the suitable governing conditions and setting the necessary boundary conditions.
4. Then the governing equations are solved. For solving these equations firstly, they are converted to the integral form and then to the linear algebraic system.
5. Finally post processing is done for analysing the visualizing the results obtained by the CFD.

The Dimensions of the geometry used for CFD analysis are:

Inner diameter of aluminium tube: 8mm

Outer diameter of tubes: 10mm

Tube thickness: 2 mm

Tube spacing: 5 mm

The meshing was done using Ansys Mesher Following are the details of the mesh:

- Meshing method used:- Tetrahedral
- Meshing size taken:- 5mm
- Number of inflation layers used:- 5 (programme controlled method)
- Number of elements: 32818

- Total number of nodes : 12482
- Average Skewness : 0.25 (generally should not exceed 1 for a good quality mesh)

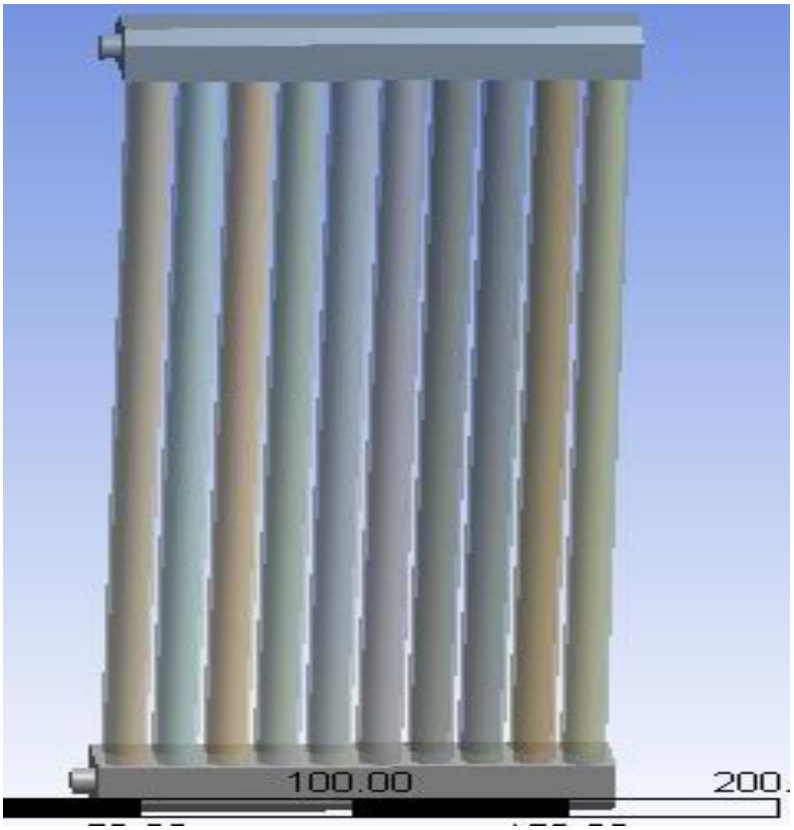

Figure 6.11: Modelling of Radiator

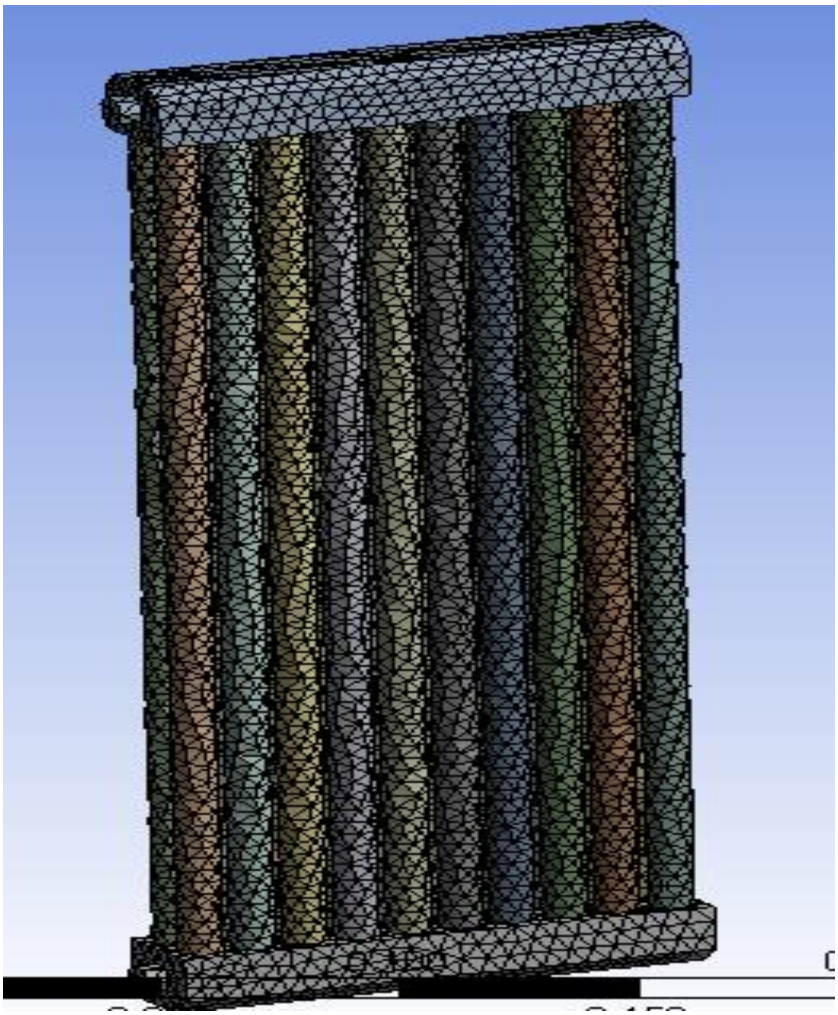

Figure 6.12: Meshing of Radiator

Modelling of the radiator is shown in Figure 6.11 and meshing of the radiator is shown in the Figure 6.12 shows the geometry divided into various number of grids. There is a term known as skewness which tells about the quality of the generated mesh. Generally, a mesh is considered to be high quality mesh if the skewness is less than1. Here, the mesh generated have the skewness less than 1.Below are the tables showing the conditions used for nanofluids and the base fluid.

Table 6.1: Ansys Conditions for water

Steps	**Selections**
Material	Fluid- Water, solid- Aluminium
Model used for base fluid	Single phase Energy equation ON Turbulence :- K-kl- omega
Inlet conditions for base fluid	Velocity Inlet 1. 0.994727m/s (Re-8734) 2. 1.16m/s (Re- 10185) 3. 1.65m/s (Re- 14556) Temp inlet- 1. 308K 2. 313 K 3. 318 K
Wall	gauge pressure zero
Outlet conditions for base fluid	Heat flux zero, No slip condition, Stationary wall

The inlet conditions i.e. temperature and velocity were kept same during the analysis for very run. The analysis for base fluid was done at three different velocities and three different mass flow rates. Nanofluids calculation is done using single phase method because if the size of nanoparticles is less than 100nm then it can be safely assumed as single phase.

Table 6.2: Ansys conditions for copper oxide nanofluids

Steps	**Selections**
Material	Fluid – copper oxide nanofluid Solid - Aluminium
Model used for copper oxide nanofluid	Single phase Turbulence model- k-kl-omega Energy equation ON
Inlet conditions for copper oxide nanofluid	Velocity Inlet (for copper oxide nanofluids) 1. 0.944m/s (Re- 8000) 2. 1.1605m/s (Re- 9800) 3. 1.6578m/s (Re- 14000) Temp- 1. 308K 2. 313K 3. 318K CuO nanofluids concentrations are 0.01%, 0.02% and 0.03%.
Outlet	gauge pressure zero
Wall	No slip condition, Stationary wall. Heat flux zero.

Table 6.3: Ansys conditions for silver coated silica nanofluid

Steps	**Selections**
Material	Fluid – Silver coated silica nanofluid Solid - Aluminium
Model used for silver coated silica nanofluid	Single phase Turbulence model- k-kl-omega Energy equation ON
Inlet conditions for silver coated silica nanofluid	Velocity Inlet (for silver coated nanofluids) 1. 0.994m/s (Re- 8500) 2. 1.1535m/s (Re- 9800) 3. 1.658m/s (Re- 14000) Temp- 1. 308K 2. 313K 3. 318K Silver coated silica nanofluids concentrations are 0.01%, 0.02% and 0.03%.
Outlet	gauge pressure zero
Wall	No slip condition, Stationary wall. Heat flux zero.

Table 6.2 and 6.3 show the different conditions used for solving nanofluid problem of both the nanofluids using ansys. The boundary conditions are taken same as that of base fluid

6.3 Data Reduction

For calculating the heat transfer coefficient and Nusselt number the following procedure has been adopted:

$$Q = h\,A\,(T_b - T_w) \tag{6.1}$$

$$Q = mC_p(T_{in} - T_{out}) \tag{6.2}$$

Where, Q is the heat transfer, m is the mass flow rate, A is the area of tube C_p is the specific heat, h is the heat transfer coefficient,T_{in} is the inlet fluid temperature,T_{out} is the fluid temperature at outlet T_b is the average inlet and outlet temperature andT_w is the average wall temperature. The temperature T_w is calculated as:

$$T_w = \frac{T_3+T_4+T_5+T_6+T_7+T_8+T_9+T_{10}}{8} \tag{6.3}$$

T_b , is calculated as

$$T_b = \frac{T_1+T_2}{2} \tag{6.4}$$

Heat transfer coefficient is calculated by,

$$h = \frac{mC_p(T_{in}-T_{out})}{A\,(T_b - T_w)} \tag{6.5}$$

Nusselt number is calculated as:

$$Nu = \frac{h\,D}{K}$$

Where, Nu is nusselt number, D is the diameter of the radiator tubes, K is the thermal conductivity of the nanofluids and h is the heat transfer coefficient

For calculating the percentage increment of heat transfer coefficient we used:

% increment = h_1-h_2/h_1*100

Where h_1 and h_2 are the heat transfer coefficients of base fluid and nanofluid respectively

Chapter 7

Results and Discussion

7.1 Experimental Results

The experimental results obtained need to be validated using standard correlations. The difference in the experimental results and the standard correlations should be within permissible range then only the setup can be considered reliable. For the set up used the calibration was done by using de-ionized water.

7.1.1 Thermal conductivity

The tables below shows the thermal conductivity of both the nanofluids at various temperatures and concentrations. Table 7.1 shows the thermal conductivity of silver coated silica nanofluids and the thermal conductivity of copper oxide nanofluids

Temperature and particle volume fraction	K of copper oxide nanofluid	K of silver coated silica nanofluid
30℃		
0.01 %	0.411	0.583
0.02 %	0.432	0.596
0.03%	0.449	0.607
40℃		
0.01%	0.500	0.6653

0.02%	0.506	0.6796

0.03%	0.521	0.6873
45℃		
0.01%	0.553	0.7724
0.02%	0.564	0.7855
0.03%	0.567	0.843

Table 7.1 Variation of Thermal conductivity of silver coated silica nanofluids and copper oxide nanofluid with temperature and particle volume fraction

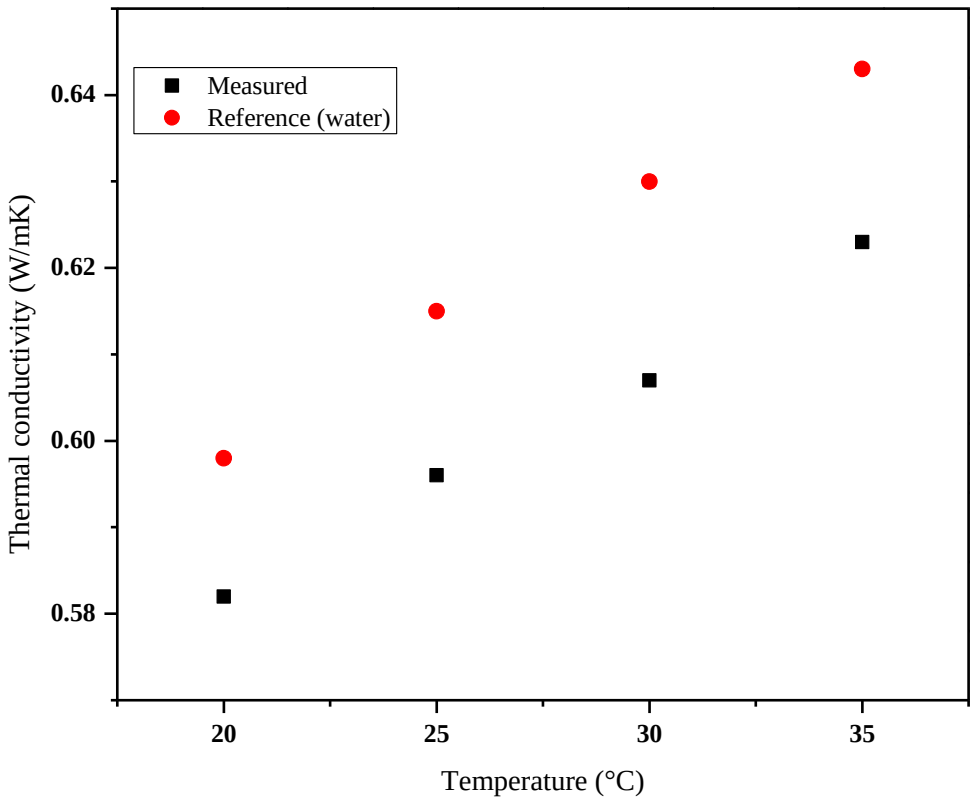

Figure 7.1: Comparison between thermal conductivity of measured data and water (standard)

Figure 7.1 shows the thermal conductivity of water measured by KD2 Pro and its comparison with the reference data. The figures 7.1 and 7.2 show the comparison of thermal conductivity of both the nanofluids with that of theoretical correlations. It can be seen in Fig 7.1 that the Yu and Choi model predicts the thermal conductivity of the copper oxide nanofluids quiet well whereas in fig 7.2 we can see that no model is able to predict the thermal conductivity of silver coated silica nanofluids. However, the Wasp model gives the results somewhat closer to that of exact

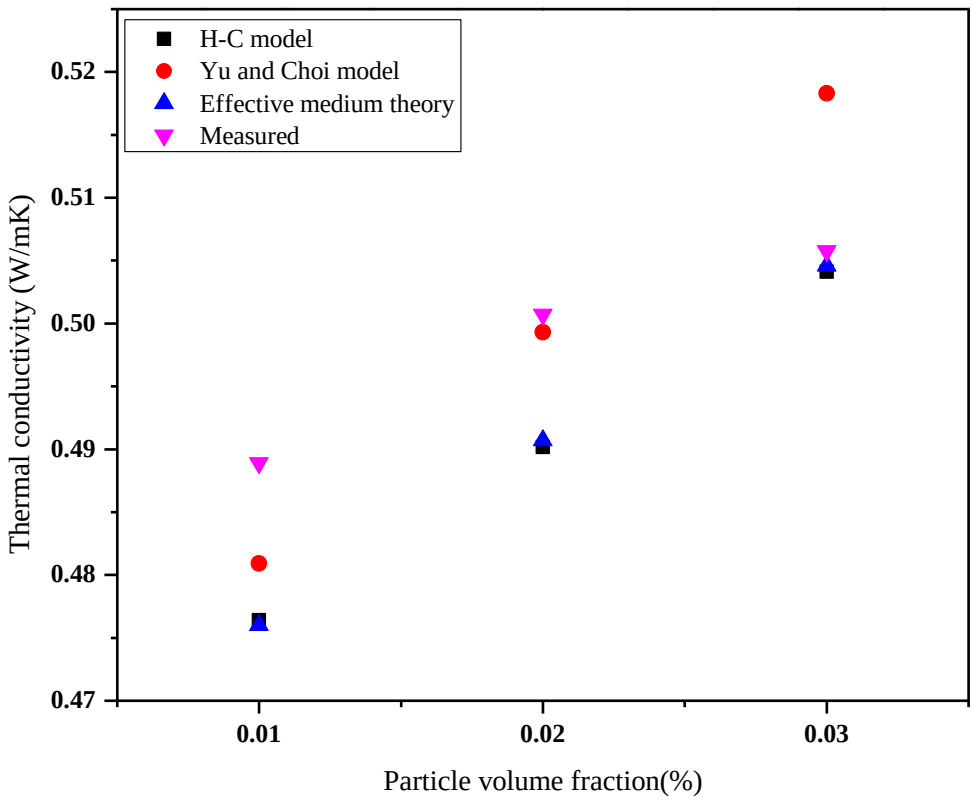

Fig.7.2. Comparison of thermal conductivity between measured data of Copper oxide nanofluids and data obtained from correlations

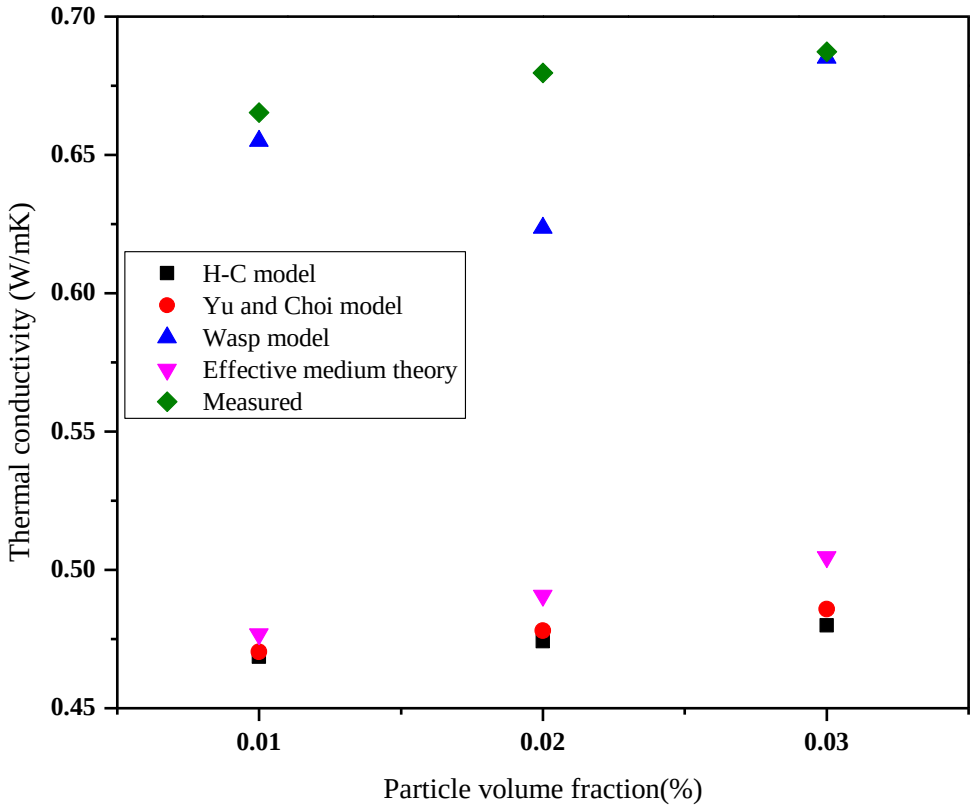

Fig.7.3. Comparison of thermal conductivity between measured data of silver coated silica nanofluids and data obtained from correlations

7.1.2 Heat transfer coefficient

The heat transfer coefficient of both the nanofluids are measured at 40°c and at three different mass flow rates i.e. 3, 3.5, 5 lpm. In order to validate the experimental set up, water is used first at similar conditions. The experimental results are compared with that of Gnielinski equation [16], as it the best equation as per our experimental conditions. It is given as:

$$\mathrm{Nu} = \frac{\left(\frac{f}{8}\right)(Re-1000)Pr}{1+12.7\left(\frac{f}{8}\right)^{0.5}\left(Pr^{\frac{2}{3}}-1\right)} \qquad (7.1)$$

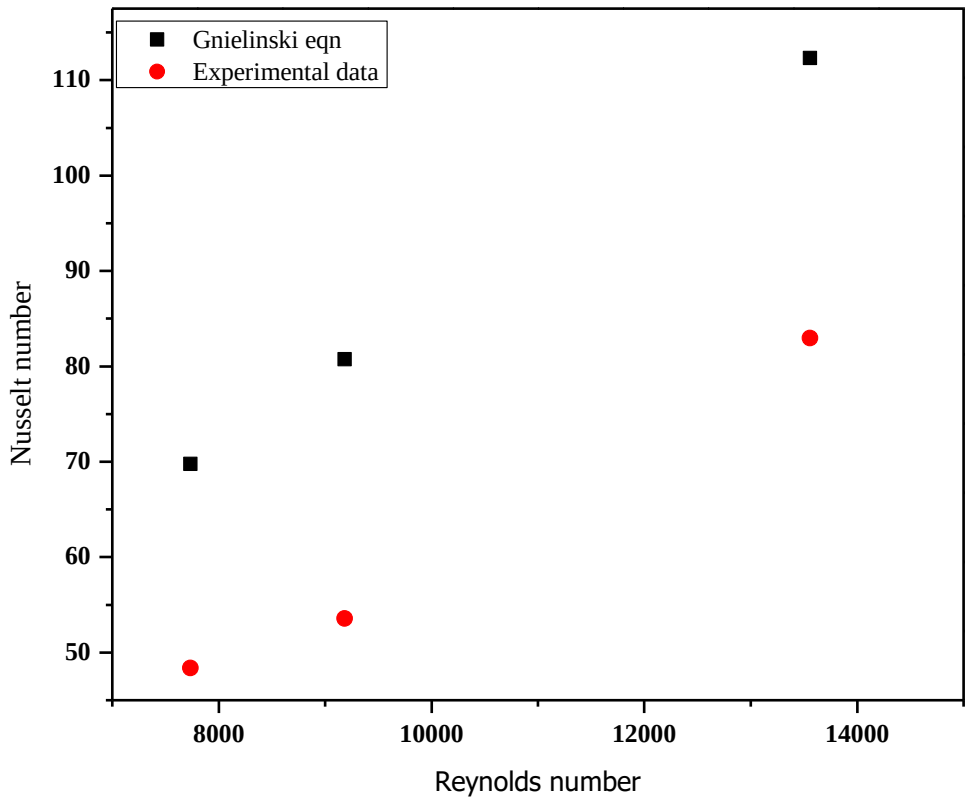

Fig.7.4. Nusselt number comparison between calculated values and values from Gnielinski equation

The results show a good agreement with that of Gnielinski equation as shown in figure 7.4. The heat transfer coefficient and the Nusselt number of the nanofluids are higher than those of base fluid and they further increase with particle volume fraction, mass flow rate and Reynolds number.

The experimental results matches well with that of Gnielinski equation which means the experimental set up can be used for nanofluids also. The experimental results of nanofluids are validated by the equations below:

The Dittus bolter correlation [17] can be defined as:

$$Nu_{nf} = 0.021\, {Re^{0.8}}_{nf}\, {Pr^{0.5}}_{nf} \qquad (7.2)$$

The Xuan and li correlation [18] can be defines as

$$Nu_{nf} = 0.0059(1.0 + 7.6286\emptyset^{0.6886})Re^{0.9238}{}_{nf}Pr^{0.4}{}_{nf} \quad (7.3)$$

The Reynolds number for nanofluids is given as

$$Re_{nf} = \frac{\rho_{nf} u_m D}{\mu_{nf}} \quad (7.4)$$

The peclet and prandtl number of the nanofluids can be given as

$$Pe_{nf} = \frac{U_{nf}}{Dp_{nf} \propto_{nf}} \quad (7.5)$$

$$Pr_{nf} = \frac{\mu_{nf}\ cp_{nf}}{K_{nf}} \quad (7.6)$$

Here d_p is the diameter of the nanoparticles and the thermal diffusivity of the nanofluids can be calculated as:

$$\propto_{nf} = \frac{K_{nf}}{\rho_{nf} Cp_{nf}} \quad (7.7)$$

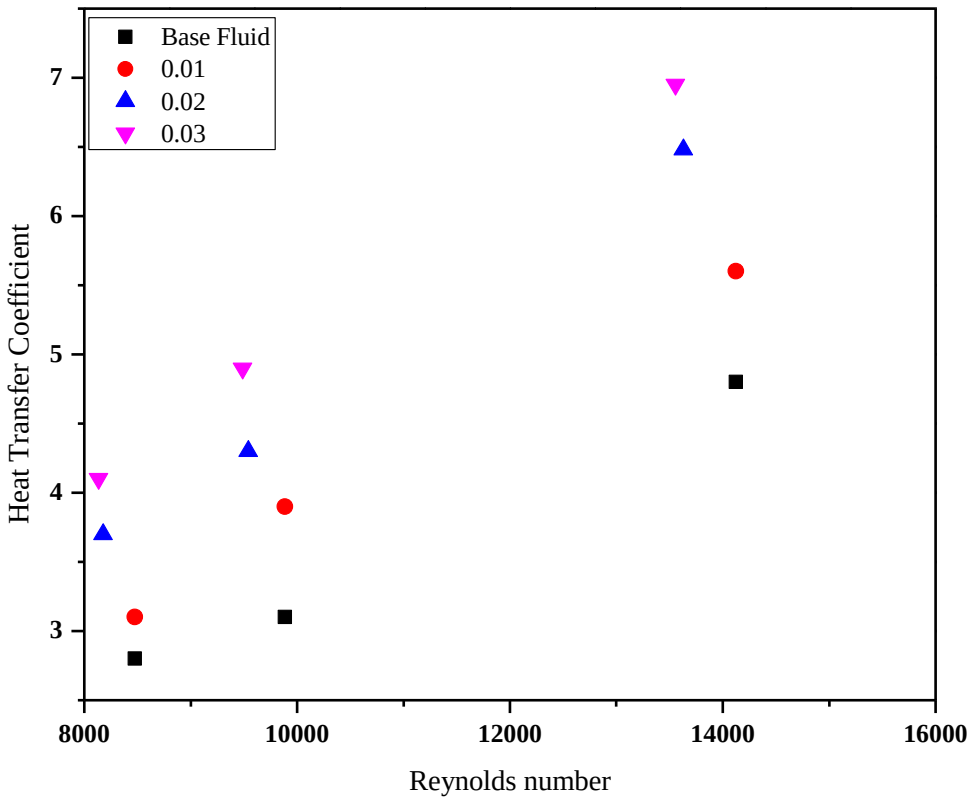

Fig.7.5. Heat transfer coefficient versus Reynolds number of copper oxide nanofluids at different volume concentration

The figure 7.5 shows the variation of heat transfer coefficient of copper oxide nanofluids with that of Reynolds number at different particle volume concentration i.e. 0.01, 0.02 and 0.03% and at different mass flow rates of 3, 3.5, 5 lpm. It can be seen that with increase in mass flow rate and particle volume fraction, the heat transfer coefficient increases. The abrupt rise in heat transfer coefficient can be seen when the mass flow rate changes 3.5lpm to 5lpm.

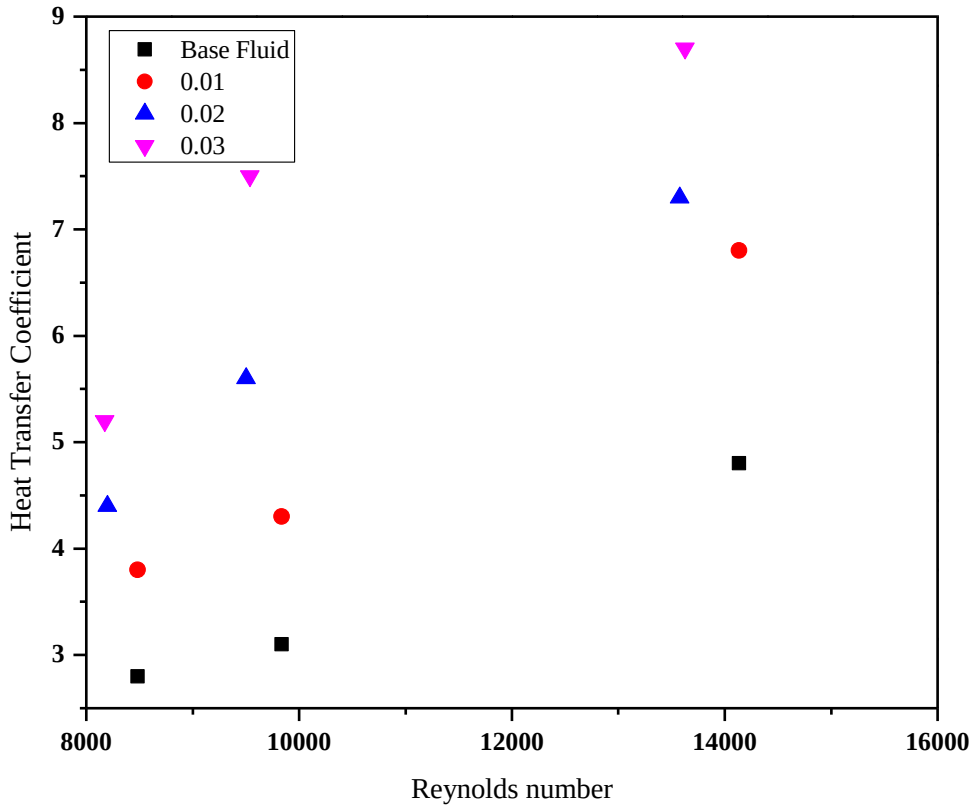

Fig.7.6. Heat transfer coefficient versus Reynolds number of silver coated silica nanofluids at different volume concentration

The figure 7.6 shows the variation of heat transfer coefficient of silver coated silica nanofluids with that of Reynolds number at different particle volume concentration i.e. 0.01, 0.02 and 0.03% and at different mass flow rates of 3, 3.5, 5 lpm. It can be seen that with increase in mass flow rate and particle volume fraction, the heat transfer coefficient increases. The abrupt rise in heat transfer coefficient can be seen when the mass flow rate changes 3.5lpm to 5lpm.

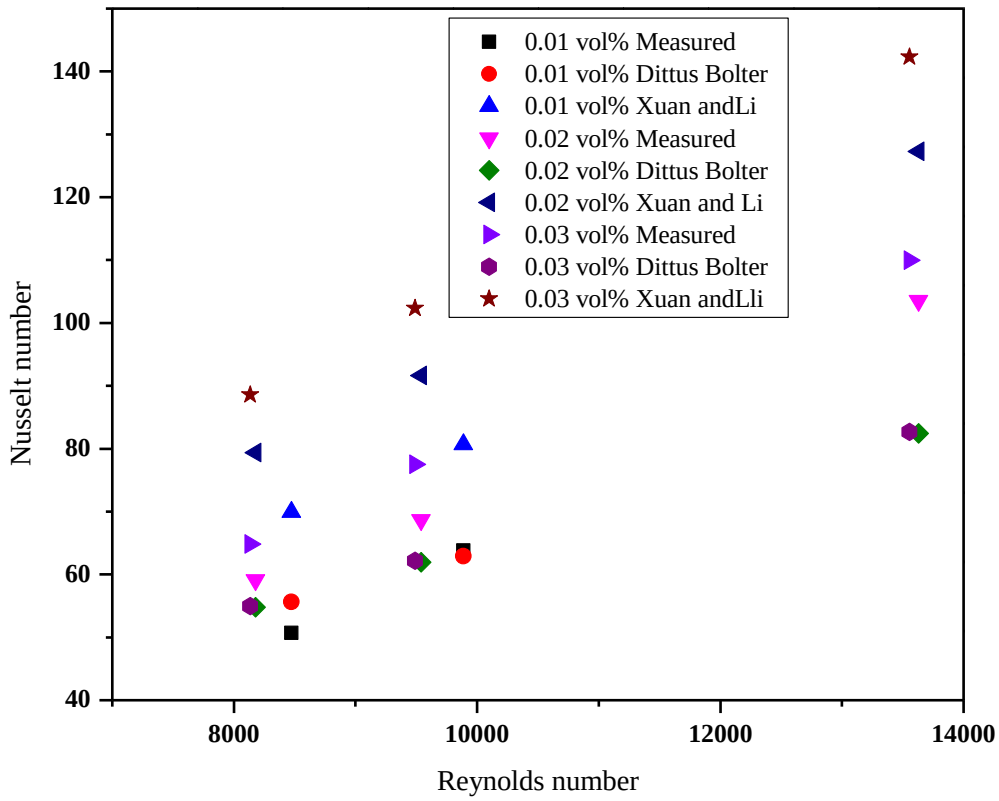

Fig.7.7. Nusselt number versus Reynolds number of copper oxide nanofluids at different volume concentration of the measured data and calculated from correlations

The Figure 7.7 shows the variation of Nusselt number of copper oxide nanofluids with that of Reynolds number, it can be seen that with an increase in Reynolds number and particle volume fraction the Nusselt number increases. The figure also shows the comparison of the measured Nusselt number results with that of the calculated from the theoretical correlations. The comparison was made with two correlations i.e. Dittus Bolter and Xuan and Li. The Dittus Bolter correlation predicts the Nusslet number quiet well, whereas the Xuan and Li correlation over predicts the Nusslet number.

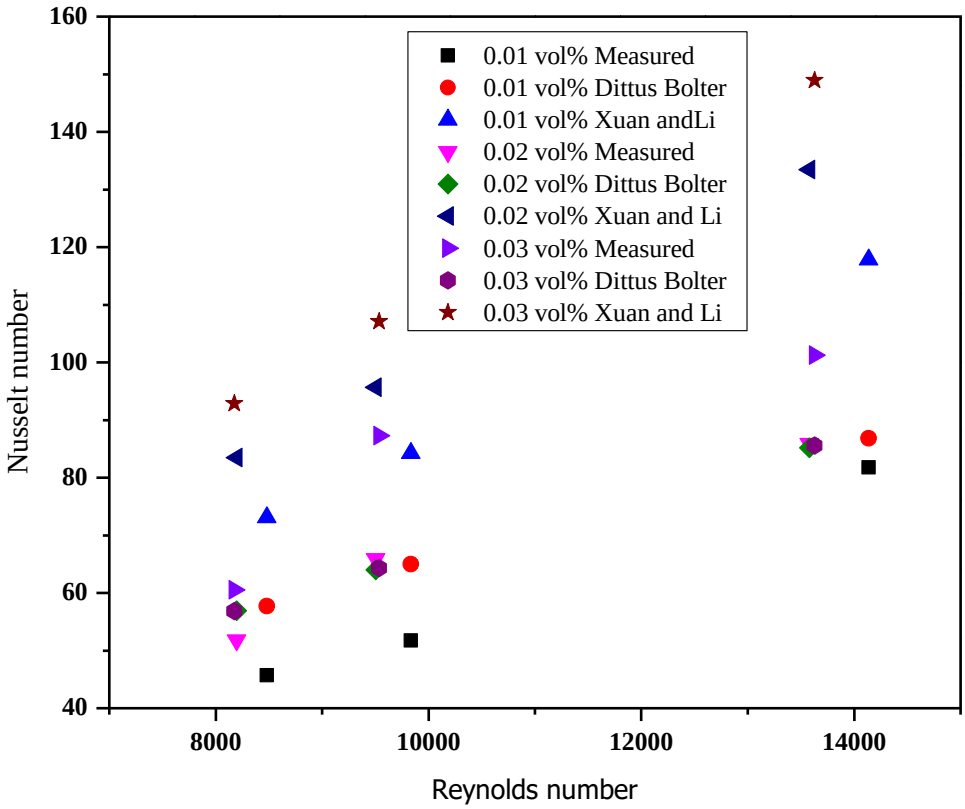

Fig.7.8. Nusselt number versus Reynolds number of silver coated silica nanofluids at different volume concentration of the measured data and calculated from correlations

The Figure 7.8 shows the variation of Nusselt number of silver coated silica nanofluids with that of Reynolds number, it can be seen that with an increase in Reynolds number and particle volume fraction the Nusselt number increases. The figure also shows the comparison of the measured Nusselt number results with that of the calculated from the theoretical correlations. The comparison was made with two correlations i.e. Dittus Bolter and Xuan and Li. The Dittus Bolter correlation predicts the Nusslet number quiet well, whereas the Xuan and Li correlation over predicts the Nusslet number.

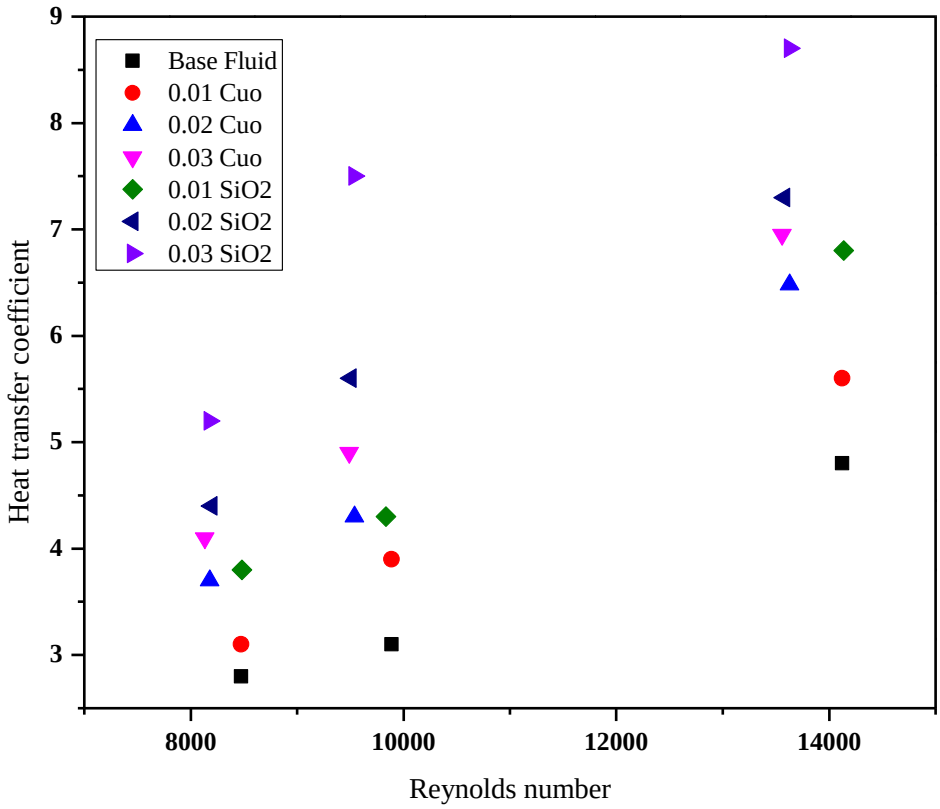

Fig.7.9. Heat transfer coefficient comparison of both the nanofluids

The figure 7.9 shows the comparison of heat transfer coefficient of both the nanofluids i.e. copper oxide and silver coated silica. The difference in heat transfer coefficient at 0.01 and 0.02% volume concentration is not much but the difference is pretty high at 0.03% volume concentration especially at 5 lpm mass flow rate.

7.2 CFD Results

7.2.1 Comparison of experimental and CFD results

As mentioned above the CFD results are not fully reliable due to the various approximations taken. So, the CFD results need to be compared with that of experimental results for validation. The figure 7.10 and 7.11 shows the comparison of CFD results and experimental results. The agreement for both the nanofluids is quiet good which shows that the CFD results are reliable for our case.

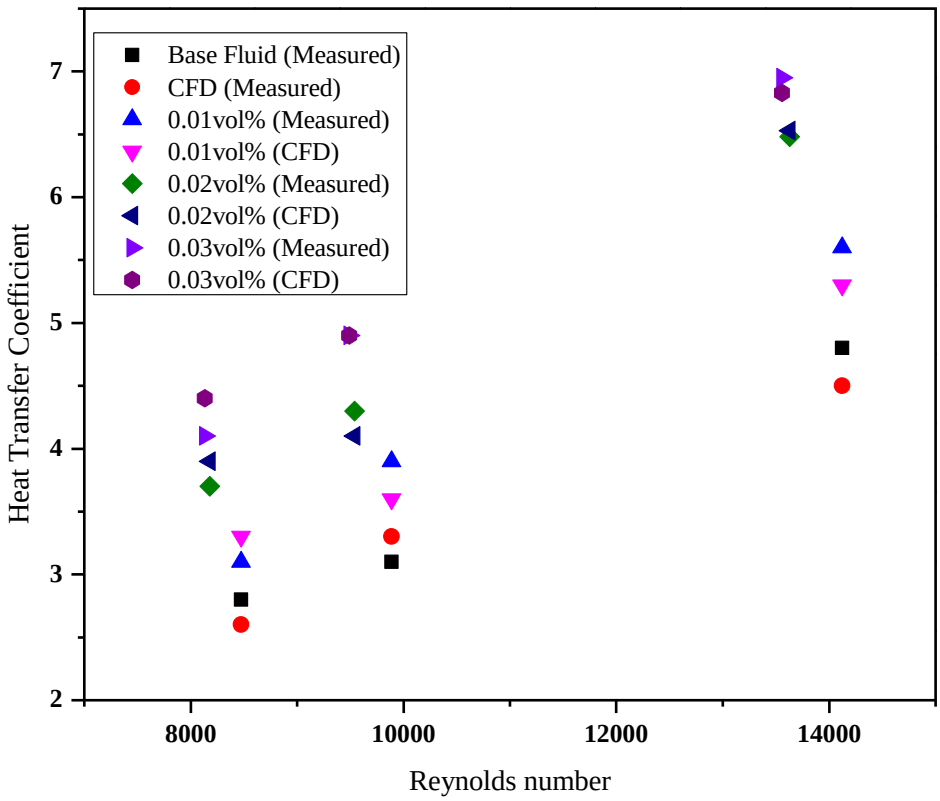

Fig.7.10. Heat transfer coefficient comparison for copper oxide nanofluid of CFD and experimental results

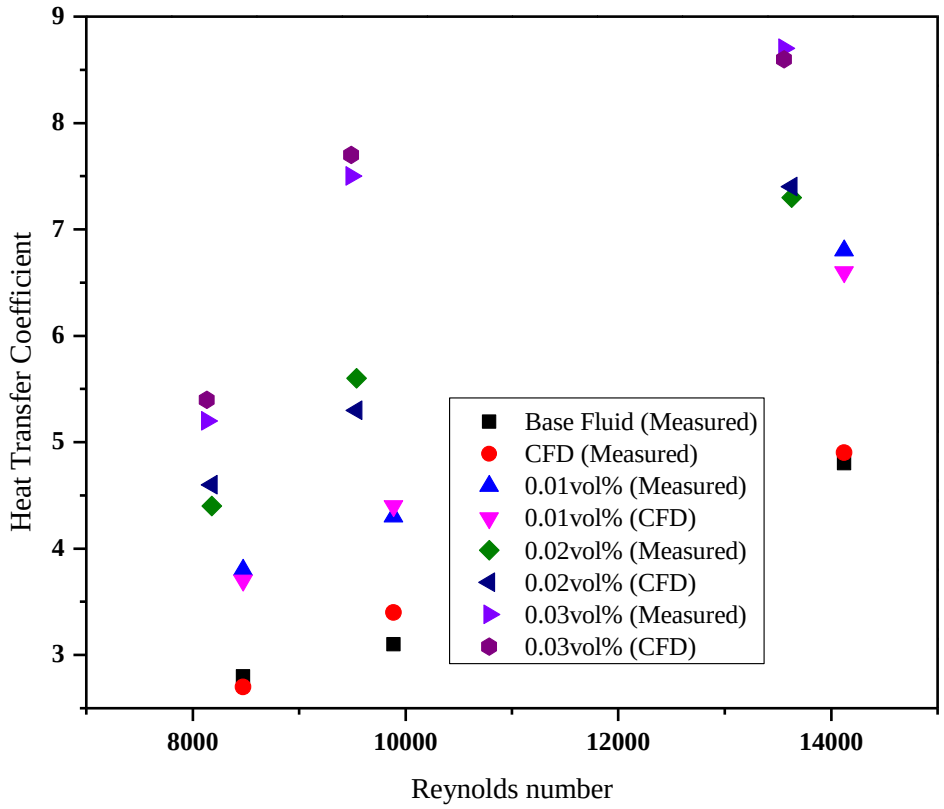

Fig.7.11. Heat transfer coefficient comparison for silver coated silica nanofluid of CFD and experimental results

Figure 7.12 shows the temperature contours i.e. how the temperature of the fluid varies with the length of the radiator tube. The colour change from red to orange and then to yellow shows the temperature fall of the fluid. The left hand side shows the scale of the temperature variation.

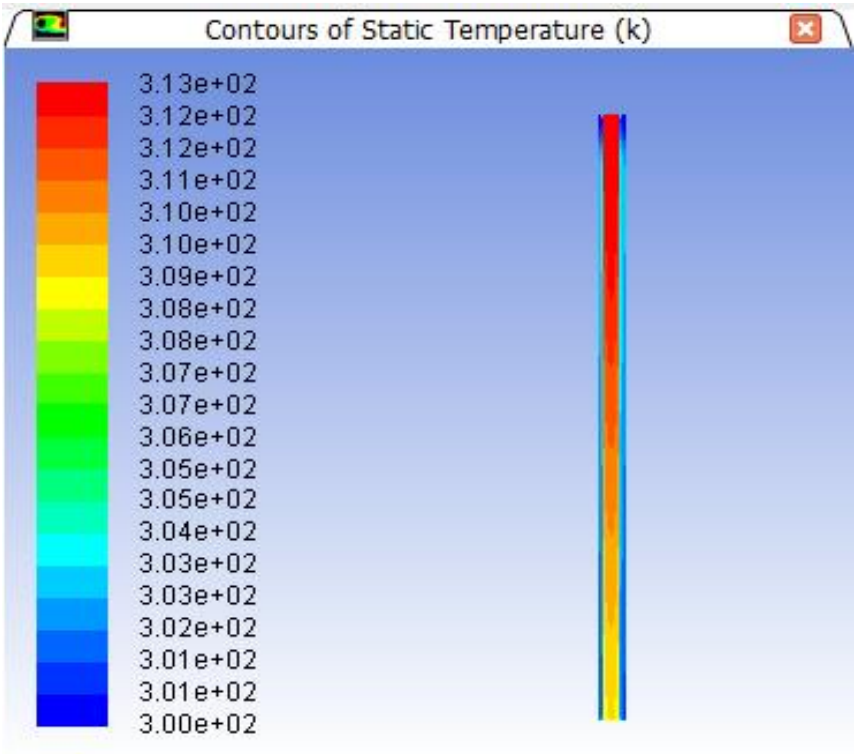

Fig.7.12. Contours of Temperature

Chapter 8

Conclusions and Future Scope

8.1 Conclusions

1. So, we can conclude that the heat transfer coefficient and the Nusselt number of the nanofluids are higher than those of base fluid and they increase with increasing the particle concentration as well as the Reynolds number. For volume concentration, 0.01% the enhancement of heat transfer coefficient of copper oxide as compared to the base fluid ranges between 9% and 32%. For 0.02%, it ranges from 21% to 37%and for 0.03%, it ranges between 14% and 31%.

2. The enhancement in heat transfer coefficient of silver coated silica nanofluids as compared to base fluid for volume concentration, 0.01% is from 26% to 46%, for 0.02% it is from 30% to 58% and for 0.03%, it is from 29% to 45% respectively.

3. Also, the hike in heat transfer coefficient by using silver coated silica nanoparticles as compared to copper oxide nanoparticles comes out to be from 20% to 35%. It can also be concluded that the volume concentration of 0.02% of silver coated silica nanofluids gives an equivalent heat transfer coefficient rise as compared to base fluid as that of 0.03% volume concentration of copper oxide silica nanofluids.

4. Moreover, the increase in thermal conductivity leads to an increase in the heat transfer performance whereas the viscosity increment of the fluid increases the boundary layer thickness, which decreases the heat transfer performance. So, at volume concentration $\leq$ 1.0vol%, the effect of thermal conductivity enhancement may overcome the effect of the viscosity increment. Moreover, the nanoparticles at higher volume concentration may form agglomerates which leads to a decrement in heat transfer coefficient.

8.2 Future Scope

1. Heat transfer coefficient is found to be increased using coated particles. So, some further substitute for these particles might increase heat transfer coefficient.

2. The nanoparticles at higher volume concentration may form agglomerates which leads to a decrement in heat transfer coefficient. So, more deep study on agglomeration is required.

References

Masuda, H., Ebata, A. and Teramae, K., 1993. Alteration of thermal conductivity and viscosity of liquid by dispersing ultra-fine particles. Dispersion of Al2O3, SiO2 and TiO2 ultra-fine particles.

Choi, S. U. S., 1995, "Enhancing Thermal Conductivity of Fluids with Nanoparticles," *Developments and Applications of Non-Newtonian Flows*, D. A. Siginer, and H. P. Wang, eds., The American Society of Mechanical Engineers, New York, **FED-Vol. 231 / MD-Vol.66**, pp. 99-105.

Chein, R. and Chuang, J., 2007. Experimental microchannel heat sink performance studies using nanofluids. *International Journal of Thermal Sciences*, *46*(1), pp.57-66.

Lee, J. and Mudawar, I., 2007. Assessment of the effectiveness of nanofluids for single-phase and two-phase heat transfer in micro-channels. *International Journal of Heat and Mass Transfer*, *50*(3), pp.452-463.

Eastman, J.A., Choi, S.U.S., Li, S., Yu, W. and Thompson, L.J., 2001. Anomalously increased effective thermal conductivities of ethylene glycol-based nanofluids containing copper nanoparticles. *Applied physics letters*, *78*(6), pp.718-720.

Yu, W., France, D.M., Routbort, J.L. and Choi, S.U., 2008. Review and comparison of nanofluid thermal conductivity and heat transfer enhancements. *Heat Transfer Engineering*, *29*(5), pp.432-460.

Parker, J.C., Brotzman Jr, R.W. and Ali, M.N., 1996. Coating opportunities for nanoparticles made from the condensation of physical vapors. *MATERIAL AND MANUFACTURING PROCESS*, *11*(2), pp.263-270.

Chon, C.H., Kihm, K.D., Lee, S.P. and Choi, S.U., 2005. Empirical correlation finding the role of temperature and particle size for nanofluid (Al 2 O 3) thermal conductivity enhancement. *Applied Physics Letters*, *87*(15), p.153107.

Das, S.K., Putra, N., Thiesen, P. and Roetzel, W., 2003. Temperature dependence of thermal conductivity enhancement for nanofluids. *Journal of heat transfer*, *125*(4), pp.567-574

Li, C.H. and Peterson, G.P., 2006. Experimental investigation of temperature and volume fraction variations on the effective thermal conductivity of nanoparticle suspensions (nanofluids). *Journal of Applied Physics*, *99*(8), p.084314.

Pak, B.C. and Cho, Y.I., 1998. Hydrodynamic and heat transfer study of dispersed fluids with submicron metallic oxide particles. *Experimental Heat Transfer an International Journal*, *11*(2), pp.151-170.

Hwang, K.S., Jang, S.P. and Choi, S.U., 2009. Flow and convective heat transfer characteristics of water-based Al 2 O 3 nanofluids in fully developed laminar flow regime. *International journal of heat and mass transfer*, *52*(1), pp.193-199.

Heris, S.Z., Esfahany, M.N. and Etemad, S.G., 2007. Experimental investigation of convective heat transfer of Al 2 O 3/water nanofluid in circular tube. *International Journal of Heat and Fluid Flow*, *28*(2), pp.203-210.

Heris, S.Z., Etemad, S.G. and Esfahany, M.N., 2006. Experimental investigation of oxide nanofluids laminar flow convective heat transfer. *International Communications in Heat and Mass Transfer*, *33*(4), pp.529-535.

Putra, N., Thiesen, P. and Roetzel, W., 2003. Temperature dependence of thermal conductivity enhancement for nanofluids. *J Heat Transf*, *125*, pp.567-574.

Li, Q., Xuan, Y. and Wang, J., 2003. Investigation on convective heat transfer and flow features of nanofluids. *Journal of Heat transfer*, *125*(2003), pp.151-155.

Jang, S.P. and Choi, S.U., 2004. Role of Brownian motion in the enhanced thermal conductivity of nanofluids. *Applied physics letters*, *84*(21), pp.4316-4318.

Murshed, S.M.S., Leong, K.C. and Yang, C., 2005. Enhanced thermal conductivity of TiO2—water based nanofluids. *International Journal of thermal sciences*, *44*(4), pp.367-373.

Evans, W., Fish, J. and Keblinski, P., 2006. Role of Brownian motion hydrodynamics on nanofluid thermal conductivity. *Applied Physics Letters*, *88*(9), p.093116.

Hong, K.S., Hong, T.K. and Yang, H.S., 2006. Thermal conductivity of Fe nanofluids depending on the cluster size of nanoparticles. *Applied Physics Letters*, *88*(3), p.031901.

Beck, M.P., Yuan, Y., Warrier, P. and Teja, A.S., 2009. The effect of particle size on the thermal conductivity of alumina nanofluids. *Journal of Nanoparticle Research*, *11*(5), pp.1129-1136.

Kole, Madhusree, and T. K. Dey. "Viscosity of alumina nanoparticles dispersed in car engine coolant." *Experimental Thermal and Fluid Science* 34, no. 6 (2010): 677-683.

Leong, K.Y., Saidur, R., Kazi, S.N. and Mamun, A.H., 2010. Performance investigation of an automotive car radiator operated with nanofluid-based coolants (nanofluid as a coolant in a radiator). *Applied Thermal Engineering*, *30*(17), pp.2685-2692.

Kole, M. and Dey, T.K., 2010. Thermal conductivity and viscosity of Al2O3 nanofluid based on car engine coolant. *Journal of Physics D: Applied Physics*, *43*(31), p.315501.

Vaisi, A., Esmaeilpour, M. and Taherian, H., 2011. Experimental investigation of geometry effects on the performance of a compact louvered heat exchanger. *Applied Thermal Engineering*, *31*(16), pp.3337-3346.

Peyghambarzadeh, S.M., Hashemabadi, S.H., Hoseini, S.M. and Jamnani, M.S., 2011. Experimental study of heat transfer enhancement using water/ethylene glycol based nanofluids as

a new coolant for car radiators. *International Communications in Heat and Mass Transfer*, *38*(9), pp.1283-1290.

Peyghambarzadeh, S.M., Hashemabadi, S.H., Jamnani, M.S. and Hoseini, S.M., 2011. Improving the cooling performance of automobile radiator with Al 2 O 3/water nanofluid. *Applied Thermal Engineering*, *31*(10), pp.1833-1838.

Warrier, P. and Teja, A., 2011. Effect of particle size on the thermal conductivity of nanofluids containing metallic nanoparticles. *Nanoscale research letters*, *6*(1), p.247.

Murshed, S.M., de Castro, C.A. and Lourenco, M.J.V., 2012. Effect of surfactant and nanoparticle clustering on thermal conductivity of aqueous nanofluids. *Journal of Nanofluids*, *1*(2), pp.175-179.

Azizian, R., Doroodchi, E. and Moghtaderi, B., 2012. Effect of nanoconvection caused by Brownian Motion on the enhancement of thermal conductivity in nanofluids| NOVA. The University of Newcastle's Digital Repository.

Arani, A.A. and Amani, J., 2012. Experimental study on the effect of TiO 2–water nanofluid on heat transfer and pressure drop. *Experimental Thermal and Fluid Science*, *42*, pp.107-115.

Abd, A.K., Al-Jabair, S. and Sultan, K., 2012. Experimental investigation of heat transfer and flow of nano fluids in horizontal circular tube. In *Proceedings of World Academy of Science, Engineering and Technology* (No. 61). World Academy of Science, Engineering and Technology.

Naraki, M., Peyghambarzadeh, S.M., Hashemabadi, S.H. and Vermahmoudi, Y., 2013. Parametric study of overall heat transfer coefficient of CuO/water nanofluids in a car radiator. *International Journal of Thermal Sciences*, *66*, pp.82-90.

Hussein, A.M., Sharma, K.V., Bakar, R.A. and Kadirgama, K., 2013. The effect of cross sectional area of tube on friction factor and heat transfer nanofluid turbulent flow. *International Communications in Heat and Mass Transfer*, *47*, pp.49-55.

Sarkar, J. and Tarodiya, R., 2013. Performance analysis of louvered fin tube automotive radiator using nanofluids as coolants. *International Journal of Nanomanufacturing*, *9*(1), pp.51-65.

Teng, T.P. and Yu, C.C., 2013. Heat dissipation performance of MWCNTs nano-coolant for vehicle. *Experimental Thermal and Fluid Science*, *49*, pp.22-30.

Peyghambarzadeh, S.M., Hashemabadi, S.H., Naraki, M. and Vermahmoudi, Y., 2013. Experimental study of overall heat transfer coefficient in the application of dilute nanofluids in the car radiator. *Applied Thermal Engineering*, *52*(1), pp.8-16.

Bozorgan, N., Krishnakumar, K. and Bozorgan, N., 2013. The Performance Evaluation of Overall Heat Transfer and Pumping Power of γ-Al 2 O 3/water Nanofluid as Coolant in Automotive Diesel Engine Radiator. *Analele Universitatii'Eftimie Murgu'*, *20*(1).

LotfizadehDehkordi, B., Kazi, S.N., Hamdi, M., Ghadimi, A., Sadeghinezhad, E. and Metselaar, H.S.C., 2013. Investigation of viscosity and thermal conductivity of alumina nanofluids with addition of SDBS. *Heat and Mass Transfer*, *49*(8), pp.1109-1115.

Hussein, A.M., Bakar, R.A. and Kadirgama, K., 2014. Study of forced convection nanofluid heat transfer in the automotive cooling system. *Case Studies in Thermal Engineering*, *2*, pp.50-61.

Chavan, D. and Pise, A.T., 2014. Performance investigation of an automotive car radiator operated with nanofluid as a coolant. *Journal of Thermal Science and Engineering Applications*, *6*(2), p.021010.

Vermahmoudi, Y., Peyghambarzadeh, S.M., Hashemabadi, S.H. and Naraki, M., 2014. Experimental investigation on heat transfer performance of/water nanofluid in an air-finned heat exchanger. *European Journal of Mechanics-B/Fluids*, *44*, pp.32-41.

Hussein, A.M., Bakar, R.A. and Kadirgama, K., 2014. Study of forced convection nanofluid heat transfer in the automotive cooling system. *Case Studies in Thermal Engineering*, *2*, pp.50-61

Chougule, S.S. and Sahu, S.K., 2014. Comparative study of cooling performance of automobile radiator using Al2O3-water and carbon nanotube-water nanofluid. *Journal of Nanotechnology in Engineering and Medicine*, *5*(1), p.010901.

F.P. Incropera, D.P. DeWitt, Fundamentals of Heat and Mass Transfer, Springer,1996

Gnielinski, V., 1976. New equations for heat and mass-transfer in turbulent pipe and channel flow. *International chemical engineering*, *16*(2), pp.359-368.

Xuan, Y. and Li, Q., 2000. Heat transfer enhancement of nanofluids. *International Journal of heat and fluid flow*, *21*(1), pp.58-64

Adams, T.M., Abdel-Khalik, S.I., Jeter, S.M. and Qureshi, Z.H., 1998. An experimental investigation of single-phase forced convection in microchannels. *International Journal of Heat and Mass Transfer*, *41*(6-7), pp.851-857.